REACTIVITY OF OXYGEN SPECIES IN HOMOGENEOUS AND HETEROGENEOUS AQUEOUS ENVIRONMENTS

By

OLHA FURMAN

A dissertation submitted in partial fulfillment of
the requirements for the degree of

DOCTOR OF PHILOSOPHY

WASHINGTON STATE UNIVERSITY
Department of Civil and Environmental Engineering

August 2009

To the Faculty of Washington State University:

The members of the Committee appointed to examine the dissertation of OLHA FURMAN find it satisfactory and recommend that it be accepted.

Richard J. Watts, Ph.D., Chair

David R. Yonge, Ph.D.

Marc W. Beutel, Ph.D.

I. Francis Cheng, Ph.D.

ACKNOWLEDGEMENT

I would like to express my gratitude to my advisor Dr. Richard Watts for his ideas, guidance and support. I would like to thank my committee members: Dr. Frank Cheng, Dr. Marc Beutel and Dr. Dave Yonge for their time and input. I would like to thank Dr. Amy Teel for her ideas and help to improve my writing. I am thankful to Dr. Frank Cheng' research group: Alexander Blumenfeld, Derek Laine, Kenichi Shimizu for their help with ESR spectroscopy and modeling. I would like to thank Dr. Rosen for synthesizing and sending a spin trap BMPO to our laboratory. I am thankful to Dr. Dave Evans and Ben Harlow for their support to develop methodology in the isotope laboratory. I would like to thank Dr. Tom Jobson and Lee Bamesberger for answering my questions.

I was lucky to be surrounded by nice people in Dr.Watts' research group. I would like to express special thanks to Dennis Finn and Robert Vaughan, past laboratory managers, and Mushtaque Ahmad who is currently managing Dr.Watts' laboratory. I had a good time working together with Megan, Joseph, Josh, Mike, Jeremiah, Marissa, Joe, Ana, and Maggie. I am thankful to Pablo Escobedo for his help with SEM and his support. I would like to express gratitude to my parents Nadiya Furman and Sergiy Furman for their love and understanding. I am thankful to my friend Yevhen Sahan for his support and understanding.

REACTIVITY OF OXYGEN SPECIES IN HOMOGENEOUS AND HETEROGENEOUS AQUEOUS ENVIRONMENTS

Abstract

by Olha Furman, Ph.D.
Washington State University
August 2009

Chair: Richard J. Watts

Three different topics related to the reactivity of oxygen species in homogenous and heterogeneous aqueous environments were studied. An introduction that covers theory and motivation for the research is presented in the first chapter. The second and third chapters examine superoxide reactivity in water-aprotic solvent and water-solid mixtures, respectively. Superoxide species are of interest in environmental chemistry because they have potential to destroy highly oxidized organic chemicals such as chlorinated solvents, pesticides, dioxins and other chemicals that are carcinogenic in majority cases. Superoxide is a strong nucleophile in organic solvents; however, it shows a significantly lower reactivity in aqueous systems. The results of the first phase of research revealed that increasing amounts of water added to nonaqueous systems decreased the activity of superoxide in the nonaqueous media, but enough activity remained for effective treatment. Superoxide was then generated in the aqueous phase of two-phase water–organic media systems, and significant superoxide activity was achieved in the organic media with the addition of phase transfer catalysts (crown ether and polyethylene glycol) to transfer superoxide into the nonaqueous phase. The results of this research demonstrate that superoxide that is generated in water photochemically, electrochemically, or through the

catalytic decomposition of peroxygens has the potential to be transferred to oils, sludges, and other less toxic nonaqueous media to destroy highly refractory contaminants such as PCDDs.

The results of the second phase of study on superoxide reactivity in water-solid matrices showed that similar to the addition of solvents, the presence of solid surfaces also enhances the reactivity of superoxide in water, possibly by altering the superoxide solvation shell. Linear relations were found between superoxide reactivity and surface area of the solids in aqueous solutions.

The third phase of research elucidates the mechanism of base activated persulfate system, which has important implications for groundwater and soil treatment processes. A mechanism for base activated persulfate was proposed in which 1) persulfate decomposes to hydroperoxide through alkaline hydrolysis, and 2) hydroperoxide reduce another persulfate molecule resulting in the formation of sulfate radical and sulfate; the hydroperoxide is then oxidized to superoxide.

TABLE OF CONTENTS

LIST OF TABLES

CHAPTER 1: INTRODUCTION

LIST OF FIGURES

CHAPTER 1: INTRODUCTION

CHAPTER 2: VOLUME REDUCTION OF NONAQUEOUS MEDIA CONTAMINATED WITH PCDDs ASSOCIATED WITH PESTICIDE WASTE USING SUPEROXIDE

CHAPTER 3: ENHANCED REACTIVITY OF SUPEROXIDE IN WATER-SOLID MATRICES

CHAPTER 4: MECHANISM OF BASE-ACTIVATION OF PERSULFATE

DEDICATION

This dissertation is dedicated to my mother, Nadiya Furman, my father, Sergiy Furman, and my friend Yevhen Sahan.

CHAPTER 1: INTRODUCTION

ISCO Technologies

Chlorinated organic contaminants remain an environmental and public health problem even after decades of research on processes that promote their degradation. Human and animal exposure to chlorinated aliphatic and aromatic compounds is associated with adverse health effects in the liver and thyroid, as well as dermal and ocular changes, immunological alterations, reduced birth weight, reproductive toxicity, and cancer (ATSDR 2000). Chlorinated contaminants are found in groundwater, surface water, drinking water, nonaqueous phase liquids (NAPLs), and sludges due to their use as dry-cleaners and degreasing agents, in electrical equipment, in the production of paints, plastics, coating compounds, and as flame retardants (Amend and Lederman 1992; Hitchman et al. 1995). Groundwater and soil are the most ubiquitous contaminated media (U.S. EPA 2004). Hydrophobic chlorinated organic compounds are commonly found sorbed to soils and sludges. Therefore, these chemicals are not easily degradable by natural attenuation. Numerous physical, chemical, and biological techniques have been developed for the remediation of contaminated soils, sludges, and groundwater. *In situ* treatment methods for contaminated groundwater and soils have many advantages over *ex situ* methods, including minimal disturbance, minimum equipment, and lower cost. Therefore, numerous *in situ* technologies have been developed: bioremediation, permeable reactive barriers, soil vapor extraction and air sparging for volatile organic carbons, and *in situ* chemical oxidation (Watts 1998; Watts and Teel 2006). The most widespread *ex situ* treatment technologies are incineration, solvent extraction, chemical dechlorination, advanced oxidation processes, bioremediation and electrochemical treatment (Amend and Lederman 1992; Hitchman et al. 1995; Sawyer and Martell 1992; Zhou et al. 2004).

In Situ Chemical Oxidation (ISCO) processes are widely used for the remediation of contaminated soils and groundwater. The most common oxidation treatments are catalyzed H_2O_2 propagations (CHP), permanganate, ozone, and persulfate (Watts and Teel 2006). These treatments are effective in the degradation of the majority of organic compounds: alkanes, alkenes, chlorinated organic and aromatic compounds (Table 1). For example, the hydroxyl radical generated in CHP reaction systems is a nonselective oxidant (Watts and Teel 2006). A significant advantage of CHP reactions is the reduction of highly oxidized organics and high desorption rate of contaminants from soils (Watts and Teel 2006). These phenomena are due to the generation of superoxide in CHP reactions (Watts et al. 1999). Superoxide has numerous potential applications for green chemistry and remediation: 1) *in situ* chemical treatment of soils and groundwater, 2) decontamination and recycling of process water, 3) desorption and separation of contaminants from solids and sludges for volume reduction, and 4) decolorization of textile waters for recycle. Destruction of chlorinated organic compounds by superoxide in both non-polar and polar environments was reported in numerous papers (Chern et al. 1978; Frimer and Rosenthal 1976; Lee et al. 1992; Roberts et al. 1983; Roberts and Sawyer 1981; Sawyer and Martell 1992; Smith et al. 2004; Sugimoto et al. 1987; 1988; Watts et al. 1999). Superoxide reactivity in different environments is examined in this research.

Persulfate is the newest chemical oxidant applied for ISCO purposes. Persulfate is a stable chemical, unlike hydrogen peroxide, that can be activated in the presence of soil and water. It is a strong oxidant and capable of degrading organic compounds when activated (Anipsitakis and Dionysiou 2004; Huang et al. 2005; Liang et al. 2003; 2004; Nadim et al. 2006). For example, activated persulfate was effective in destroying organic contaminants such as trichloroethylene, trichloroethane, methyl *tert*-butyl ether, polychlorinated biphenyls, and BTEX

(Liang and Bruell 2008; Liang et al. 2007; Liang et al. 2003; 2004). Base activation of persulfate is one of the most common ISCO practices, and it is examined in this research.

Superoxide Chemistry

There are numerous ways to generate superoxide: 1) direct application of potassium superoxide, 2) modified Fenton's chemistry, 3) hydrogen peroxide decomposition on the surface of metal oxides, 4) electrochemical reduction of oxygen in a solvent, 5) pulse radiolysis, and 6) photochemical generation (Afanas'ev 1989; Anpo et al. 1999; Ono et al. 1977; Sawyer and Martell 1992). The first three methods for superoxide generation are used in this study.

Application of potassium superoxide is usually used for theoretical purposes to understand the mechanisms and kinetics between superoxide and target compounds. Potassium superoxide (KO_2) is not stable in aqueous solutions and not soluble in nonpolar media; therefore, phase transfer catalysts are usually applied in nonpolar solvents. Crown ethers complex and solubilize potassium superoxide in aprotic solvents (Frimer and Rosenthal 1976; Weber and Gokel 1977). Crown ethers have been used in both solid-liquid and liquid-liquid two-phase systems (Weber and Gokel 1977). An alternative to the use of crown ethers is polyethylene glycol (PEG). PEGs can form complexes with metal cations and behave as phase transfer catalyst similar to crown ethers (Naik and Doraiswamy 1998). Polyethylene glycols are less costly, less toxic, and stable (Chen et al. 2005; Naik and Doraiswamy 1998).

The application of modified Fenton's reagent (high hydrogen peroxide concentrations and iron chelates/minerals) for the treatment of soils and groundwater has been effective in the degradation of highly oxidized contaminants and the destruction of dense nonaqueous phase liquids (DNAPLs) (Siegrist et al. 2001; Watts et al. 1999).These processes are possible due to superoxide generated in modified Fenton's systems (Watts et al. 1999):

$H_2O_2 + Fe^{3+} \longrightarrow HO_2^{\bullet} + Fe^{2+} + H^+$ [1]

$OH^{\bullet} + H_2O_2 \longrightarrow HO_2^{\bullet} + H_2O$ [2]

$HO_2^{\bullet} \longrightarrow O_2^{\bullet -} + H^+$ [3]

Several works document the formation of superoxide during hydrogen peroxide decomposition on the surface of metal oxides (Anpo et al. 1999; Kitajima et al. 1978; Ono et al. 1977). It was demonstrated that decomposition of hydrogen peroxide on metal oxides is a radical driven process (Giamello et al., 1993), and that superoxide radicals are formed in the aqueous solution (Kitajima et al., 1978; Ono et al., 1977) or at the solid surface (Anpo et al., 1999; Giamello et al., 1993). Miller and Valentine (1999) demonstrated that superoxide was formed during the surface-catalyzed decomposition of hydrogen peroxide by sand and that superoxide was capable of moving from the vicinity of the sand surface to the bulk solution. Some studies showed that superoxide was stabilized in the solid matrix as the result of the interaction of hydrogen peroxide with metal oxides (Anpo et al. 1999; Giamello et al. 1993; Zhang and Klabunde 1992). It is possible that superoxide can be deactivated by releasing an electron to the surface of the metal oxide (Ishibashi et al. 1998; Ono et al. 1977).

Watts et al. (2005a,b) demonstrated that manganese oxide-catalyzed decomposition of hydrogen peroxide at near neutral conditions generates reductants that are capable of reducing highly oxidized organics such as carbon tetrachloride. They suggested that superoxide may be responsible for the degradation of carbon tetrachloride in manganese oxide-H_2O_2 systems. The mechanisms for superoxide generation have been proposed in similar reaction systems (Hasan et al. 1999; Watts et al. 2005):

$H_2O_2 \longrightarrow H^+ + HO_2^-$ [4]

$HO_2^- \longrightarrow HO_2^{\bullet} + e^-$ [5]

$HO_2^{\bullet} \longrightarrow O_2^{\bullet -} + H^+$ [6]

$e^- + Mn^{4+} \longrightarrow Mn^{3+}$ [7]

$H^+ + Mn^{3+} \longrightarrow Mn^{4+} + H^{\bullet}$ [8]

Anpo et al. (1999):

$H_2O_2 \longrightarrow 2OH^{\bullet}$ [9]

$OH^{\bullet} + H_2O_2 \longrightarrow HO_2^{\bullet} + H_2O$ [10]

$HO_2^{\bullet} \xrightarrow{MeO} O_2^{\bullet -} + H^+$ [11]

Enhanced superoxide reactivity in the presence of catalytic and non-catalytic solid surfaces is examined in this research. Figure 1 demonstrates a simple scheme of possible superoxide pathways in the presence of solids.

Superoxide radical behaves as a nucleophile towards alkyl halides, and displaces the halide from the carbon center via an S_N2 mechanism (Sawyer and Martell 1992). Superoxide reactivity towards $RCCl_3$ compounds is consistent with the single-electron-transfer (SET) mechanism (Sawyer and Martell 1992). The reaction rate constants between superoxide and several chlorinated hydrocarbons in dimethylformamide are shown in Table 2 (Afanas'ev 1989; Sawyer and Martell 1992). Such intermediate products as peroxy compounds and alcohols were observed during the reaction between superoxide and chlorinated organic compounds (Sawyer and Martell 1992). The most common end products of the reaction between superoxide and halogenated hydrocarbons are nonhazardous carbonate, chlorine ions, and oxygen (Sawyer and Martell 1992). Highly chlorinated organics are used as probes to detect superoxide, including hexachlorobenzene ($K_{O2\bullet/[C6Cl6]} = 1\times10^3\ M^{-1}s^{-1}$) and hexachloroethane ($K_{O2-\bullet/[C2Cl6]} = 400\ M^{-1}s^{-1}$) in this study (Table 2). Carbon tetrachloride ($K_{O2-\bullet/[CCl4]} = 3.8\times10^3\ M^{-1}s^{-1}$) is more reactive with superoxide but its application is limited because of its rapid loss through volatilization.

Superoxide is a relatively stable radical and powerful nucleophile in aprotic solvents (Afanas'ev 1989; Sawyer and Martell 1992). Aqueous superoxide often acts as a one-electron reductant or as an oxidant (Sawyer and Martell 1992). However, superoxide forms hydrogen bonds in water and undergoes rapid disproportionation (Afanas'ev 1989; Bielski and Allen 1977; Marklund 1976; Sawyer and Martell 1992; Sawyer and Valentine 1981).

$2O_2^{\bullet-} + H_2O = O_2 + HO_2^- + OH^-$ [12]

Several works demonstrated that the presence of protic substrates (water, alcohol) induce the disproportionation of superoxide in aprotic solvents (Afanas'ev 1989; Andrieux et al. 1987; Che et al. 1996; Chin et al. 1982). Singh and Evans (2006) demonstrated that superoxide forms a complex with a hydrogen bond donor (water), forming HO_2^- and OH^- in a concerted process. Smith et al. (2004) showed that even dilute concentrations of solvents increased the reactivity of superoxide in water, most likely by changing its solvation shell. Superoxide reactivity in the presence of solvents less polar than water (acetone and dimethyl sulfoxide) is investigated in this study.

Persulfate Chemistry

Persulfate ion is stable in water but undergoes decomposition and activation in the presence of metals (iron, manganese, silver, cerium, cobalt and others), organic compounds (aliphatic and aromatic compounds), and under heat and light (Anipsitakis and Dionysiou 2004; House 1962; Huang et al. 2005; Kolthoff and Miller 1951; Liang and Bruell 2008; Liang et al. 2007; Liang et al. 2003; 2004; Nadim et al. 2006).

$S_2O_8^{2-} \longrightarrow 2SO_4^{\bullet-}$ (thermal/photodecomposition, reaction with organic probe) [13]

$S_2O_8^{2-} + Me^{n+} \longrightarrow SO_4^{2-} + SO_4^{\bullet-} + Me^{n+1}$ (metal activation of the persulfate) [14]

$S_2O_8^{2-} + R^{\bullet} \longrightarrow SO_4^{2-} + SO_4^{\bullet-} + R$ (reaction with organic radicals) [15]

$SO_4^{\bullet-} + H_2O \longrightarrow HSO_4^- + OH^{\bullet}$ [16]

$SO_4^{\bullet-} + OH^- \longrightarrow SO_4^{2-} + OH^{\bullet}$ [17]

Sulfate and hydroxyl radicals are formed during the thermal, photochemical, and chemical decomposition of persulfate (Anipsitakis and Dionysiou 2004; House 1962; Huang et al. 2005; Kolthoff and Miller 1951; Liang and Bruell 2008; Liang et al. 2007; Liang et al. 2003; 2004; Nadim et al. 2006). Both sulfate and hydroxyl radicals are strong oxidants. Hydroxyl radicals react with organic compounds by addition to the unsaturated bonds of alkenes and aromatic compounds and by abstracting hydrogen atoms from saturated compounds generating alkyl radicals (Walling and Johnson 1975). Sulfate radicals can also abstract hydrogen from saturated compounds and add to unsaturated or aromatic compounds (Elbenberger et al. 1977; Neta et al. 1976; Norman et al. 1970). They can also participate in electron transfer reactions with certain anions (carboxylate anion) and neutral molecules of low ionization potential (Norman et al. 1970). Sulfate radical shows a greater potential than hydroxyl radical for removing electrons from an aromatic ring (Norman et al. 1970). Reaction [17] between sulfate radical and hydroxide becomes important under basic conditions, and the ability of an organic compound to react with sulfate radical before it is hydrolyzed by hydroxide depends on the structure of the organic compound (Anipsitakis and Dionysiou 2004; Hayon et al. 1972; Norman et al. 1970). The addition of sulfate radical anion is facilitated by the presence of electron releasing groups and retarded by electron withdrawing groups (Norman et al. 1970). Table 3 lists reaction rate constants of hydroxyl and sulfate radicals with aliphatic and aromatic compounds. In general, sulfate radical is more likely to participate in electron transfer reactions, and hydroxyl radical is more likely to participate in hydrogen abstraction or addition reactions (Minisci and Citterio 1983).

Base-activated Persulfate System

Base activation is the most common activation method for persulfate ISCO. Block et al. (2004) and Root et al. (2005) demonstrated the successful destruction of chlorinated ethanes and methanes in base-activated persulfate ISCO systems. The mechanism for base activation of persulfate has not been established; some proposed mechanisms are discussed in this section.

A mechanism of persulfate decomposition in neutral and alkaline conditions was proposed by Bartlett and Cotman (1949), Gonzales and Martire (1997), and House (1962):

$S_2O_8^{2-} \xrightarrow{\text{slow}} 2SO_4^{\bullet-}$ [18]

$SO_4^{\bullet-} + OH^- \longrightarrow SO_4^{2-} + OH^{\bullet}$ $7.3 \times 10^7\ M^{-1}s^{-1}$ [19]

$SO_4^{\bullet-} + H_2O \longrightarrow HSO_4^- + OH^{\bullet}$ $<3 \times 10^3\ M^{-1}s^{-1}$ [20]

$2OH^{\bullet} \longrightarrow H_2O + 1/2\ O_2$ (termination of chain) [21]

$S_2O_8^{2-} + OH^{\bullet} \longrightarrow HSO_4^- + SO_4^{\bullet-} + \frac{1}{2}\ O_2$ [22]

$S_2O_8^{2-} + OH^{\bullet} \longrightarrow S_2O_8^- + OH^-$ (termination of chain) $10^6\ M^{-1}s^{-1}$ [23]

$SO_4^{\bullet-} + OH^{\bullet} \longrightarrow SO_4^{2-} + \frac{1}{2}\ O_2$ (termination of chain) [24]

$SO_4^{\bullet-} + S_2O_8^{2-} \longrightarrow SO_4^{2-} + S_2O_8^-$ (termination of chain) $6.3 \times 10^5\ M^{-1}s^-$ [25]

This mechanism implies that initial rate limiting step is *uv* or thermal activation [18]. In alkaline solutions sulfate radical reacts readily with hydroxide to yield hydroxyl radical [19] (Hayon et al. 1972). Oxygen is formed as a result of radical recombination [21,22,24], and the source of evolved oxygen is water (House 1962).

Singh and Venkatarao (1976) suggested the following mechanism for the decomposition of persulfate at high NaOH concentrations (~1.0M):

$S_2O_8^{2-} + OH^- \xrightarrow{\text{slow}} HSO_4^- + SO_5^{2-}$ [26]

$SO_5^{2-} \xrightarrow{\text{fast}} SO_4^{2-} + \frac{1}{2}\ O_2$ [27]

The initial reaction step is the nucleophilic attack of hydroxide ion on the S-O bond of the persulfate molecule, with the formation of peroxomonosulfate ion [26] (Singh and Venkatarao 1976). In this reaction the source of the evolved oxygen is the oxygen of the peroxide bond of the persulfate [27].

Martire and Gonzalez (1998) investigated reaction mechanisms in strong alkaline solutions of persulfate by applying photolysis. Reaction [18] is the initial rate limiting step in the study conditions, followed by reaction [19]. The hydroxyl radicals formed are scavenged by hydroxide, yielding the conjugated basic form of hydroxyl radical, $O^{\bullet -}$ [28]. $O^{\bullet -}$ radical reacts with oxygen, yielding ozonide radical [29]. The authors found that the reaction [31] between superoxide and persulfate ion can be neglected, while reactions [32-34] between $O^{\bullet -}$ and persulfate play a significant role in the study system (Martire and Gonzalez 1998). They suggested three possible reaction mechanisms [32-34] that result in the formation of peroxomonosulfate radical/ion, persulfate and sulfate radical (Martire and Gonzalez 1998).

$OH^{\bullet} + OH^{-} \longrightarrow O^{\bullet -} + H_2O$ $1.3 \times 10^{10}\ M^{-1}s^{-1}$ [28]

$O^{\bullet -} + O_2 \longrightarrow O_3^{\bullet}$ $1.3 \times 10^{10}\ M^{-1}s^{-1}$ [29]

$O_3^{\bullet -} + OH^{\bullet} \longrightarrow H^{+} + 2O_2^{\bullet -}$ $6.0 \times 10^{9}\ M^{-1}s^{-1}$ [30]

$S_2O_8^{2-} + O_2^{\bullet -} \longrightarrow SO_4^{2-} + SO_4^{\bullet -} + O_2$ $0.05\ M^{-1}s^{-1}$ [31]

$\longrightarrow SO_4^{\bullet -} + SO_5^{2-}$ [32]

$O^{\bullet -} + S_2O_8^{2-} (+H_2O) \longrightarrow SO_5^{\bullet -} + SO_4^{2-}$ [33]

$\longrightarrow S_2O_8^{\bullet -} + 2HO^{-}$ [34]

The mechanism of base-activated persulfate decomposition at relatively high persulfate and sodium hydroxide concentrations, at room temperature and without any additional activation (such as light and heat) is examined further in Chapter 4.

Objectives

The focus of the research described in this dissertation is:

- superoxide reactivity in a mixture of water and less polar solvents
- the effect of solids on superoxide reactivity in aqueous environments
- the mechanism of base-activated persulfate

This study will aid in understanding superoxide reactivity in different environments, and its application for green chemistry and the decontamination of soils, and groundwater/wastewater. Finding the mechanism of base-activated persulfate system has important implications for ISCO practices.

Scholarly Contribution

Chapter 2 has been submitted to the *Journal of Agricultural and Food Chemistry*. Chapter 3 has been published in *Environmental Science and Technology* (Furman et al. 2009), and Chapter 4 will be submitted to *Environmental Science and Technology*.

Bibliography

Afanas'ev, I. B. (1989). *Superoxide ion: chemistry and biological implication*, CRC Press, Inc, Boca Raton.

Agency for Toxic Substances and Disease Registry (ATSDR), U.S. Department of Health and Human Services, (2000). Toxicological profiles for chlorinated aliphatic and aromatic compounds, Atlanta, GA.

Amend, L. J., and Lederman, P. B. (1992). "Critical evaluation of PCB remediation technologies." *Environ. Prog.*, 11, 173-177.

Andrieux, C. P., Hapiot, P., and Saveant, J.-M. (1987). "Mechanism of superoxide ion disproportionation in aprotic solvents." *J. Am. Chem. Soc.*, 109, 3768-3775.

Anipsitakis, G. P., and Dionysiou, D. D. (2004). "Radical generation by the interaction of transition metals with common oxidants." *Environ. Sci. Technol.*, 38, 3705-3712.

Anpo, M., Che, M., Fubini, B., Garrone, E., Giamello, E., and Paganini, M. C. (1999). "Generation of superoxide ions at oxide surfaces." *Top. Catal.*, 8, 189-198.

Bartlett, P.D., and J.D. Cotman, Jr. (1949). "The kinetics of the decomposition of potassium persulfate in aqueous solutions of methanol". *J. Am. Chem. Soc.*, 71, 1419-1422.

Bielski, B. H. J., and Allen, O. (1977). "Mechanisms of the disproportionation of superoxide radicals." *J. Phys. Chem.*, 81, 1048-1050.

Block, P.A., Brown, R.A., and D. Robinson. (2004). "Novel activation technologies for sodium persulfate in situ chemical oxidation". Proceedings of the Fourth International Conference on the Remediation of Chlorinated and Recalcitrant Compounds, Monterey, CA.

Che, Y., Tsushima, M., Matsumato, F., Okajima, T., Tokuda, K., and Ohsaka, T. (1996). "Water-induced disproportionation of superoxide ion in aprotic solvents." *J. Phys. Chem.*, 100, 20134-20137.

Chen, J., Spear, S. K., Huddleston, J. G., and Rogers, R. D. (2005). "Polyethylene glycol and solutions of polyethylene glycol as green reaction media." *Green Chem.*, 7, 64-82.

Chern, C.-I., DiCosimo, R., De Jesus, R., and San Filippo, J. (1978). "A study of superoxide reactivity. Reaction of potassium superoxide with alkyl halides and tosylates." *J. Am. Chem. Soc.*, 100, 7317-7327.

Chin, D.-H., Chiericato, G., Nanni, E. J., and Sawyer, D. T. (1982). "Proton-induced disproportionation of superoxide ion in aprotic media." *J. Am. Chem. Soc.*, 104, 1296-1299.

Elbenberger H., Steenken S., O'Neill P., and Schulte-Frohlinde, D. (1978). "Pulse radiolysis and electron spin resonance studies concerning the reaction of $SO_4^{-\cdot}$ with alcohols and ethers in aqueous solution". *J. Phys. Chem.*, 82, 749-750.

Frimer, A., and Rosenthal, I. (1976). "Nucleophilic radical aromatic substitution with superoxide ion." *Tetrahedron Lett.*, 17, 2808-2812.

Furman, O., Laine, D.F., Blumenfeld, A., Teel, A.L., Shimizu, K., Cheng, I.F., and Watts, R.J. (2009). "Reactivity of superoxide in the water-solid matrices". *Environ. Sci. Technol.,* 43, 1528–1533.

Giamello, E., Calosso, L., Fubini, B., and Geobaldo, F. (1993). "Evidence of stable hydroxyl radicals and other oxygen radical species generated by interaction of hydrogen peroxide with magnesium oxide." *J. Phys. Chem.*, 97, 5735-5740.

Gonzales, M.C., and D.O. Martire. (1997). "Kinetics of $O^{\bullet-}$ and $O_3^{\bullet-}$ in alkaline aqueous solutions". *Water Sci. Technol.*, 35, 49-55.

Hayon, E., Treinin, A., and Wilf, J. (1972). "Electronic spectra, photochemistry, and autoxidation mechanism of the sulfite-bisulfite-pyrosulfite systems. The SO_2^-,SO_3^-,SO_4^-, and SO_5^- radicals." *J. Am. Chem. Soc.*, 94, 47-57.

Hitchman, M. L., Spackman, R. A., Ross, N. C., and Agra, C. (1995). "Disposal methods for chlorinated aromatic waste." *Chem. Soc. Rev.*, 24, 423-430.

House, D. A. (1962). "Kinetics and mechanism of oxidations by peroxydisulfate." *Chem. Rev.*, 62, 185-203.

Huang, K., Zhao, Z., Hoag, G., Dahmani, A., and Block, P. (2005). "Degradation of volatile organic compounds with thermally activated persulfate oxidation." *Chemosphere*, 61, 551-560.

Ishibashi, K.-I., Nosaka, Y., Hashimoto, K., and Fujishima, A. (1998). "Time-dependent behavior of active oxygen species formed on photoirradiated TiO_2 films in air." *J. Phys. Chem. B*, 102, 2117-2120.

Interstate Technology and Regulatory Council (ITRC). (2007). “Technical and Regulatory Guidance: In Situ Chemical Oxidation of Contaminated Soil and Groundwater”. Second Edition. http://www.itrcweb.org/ibt.asp

Kitajima, N., Fukuzumi, S.-I., and Ono, Y. (1978). "Formation of superoxide ion during the decomposition of hydrogen peroxide on supported metal oxides." *J. Phys. Chem.*, 82, 1505-1508.

Kolthoff, I. M., and Miller, I. K. (1951). "The chemistry of persulfate. I. The kinetics and mechanism of the decomposition of the persulfate ion in aqueous medium." *J. Am. Chem. Soc.*, 73, 3055-3059.

Lee, J. L., Yao, C. P., Wang, Y. Y., and Wan, C. C. (1992). "Electrochemical decomposition of chlorinated benzenes in dimethylformamide solvent." *Environ. Sci. Technol.*, 26, 553-556.

Liang, C., and Bruell, C. J. (2008). "Thermally activated persulfate oxidation of trichloroethylene: experimental investigation of reaction orders." *Ind. Eng. Chem. Res.,* 47, 2912-2918.

Liang, C., Wang, Z.-S., and Bruell, C. J. (2007). "Influence of pH on persulfate oxidation of TCE at ambient temperatures." *Chemosphere*, 66, 106-113.

Liang, C. J., Bruell, C. J., Marley, M. C., and Sperry, K. L. (2003). "Thermally activated persulfate oxidation of trichloroethylene (TCE) and 1,1,1-trichloroethane (TCA) in aqueous systems and soil slurries." *Soil and Sed. Contam.*, 12, 207-228.

Liang, C. J., Bruell, C. J., Marley, M. C., and Sperry, K. L. (2004). "Persulfate oxidation for in situ remediation of TCE. I. Activated by ferrous ion with and without a persulfate-thiosulfate redox couple." *Chemosphere*, 55, 1213-1223.

Marklund, S. (1976). "Spectrometric study of spontaneous disproportionation of superoxide anion radical and sensitive direct assay for superoxide dismutase." *J. Biol. Chem.*, 251, 7504-7507.

Martire, D. O., and Gonzalez, M. C. (1998). "Kinetic evidence for the reaction of $O^{-\bullet}$ radical ions and peroxodisulfate in alkaline aqueous solutions." *Int. J. Chem. Kinet.,* 30, 491-496.

Minisci, F., and Citterio, A. (1983). "Electron-transfer processes: peroxodisulfate, a useful and versatile reagent in organic chemistry." *Acc. Chem. Res.,* 16, 27-32.

Nadim, F., Huang, K., and Dahmani, A. (2006). "Remediation of soil and ground water contaminated with PAH using heat and Fe(II)-EDTA catalyzed persulfate oxidation." *Water Air Soil Pollut. Focus,* 6, 227-232.

Naik, S. D., and Doraiswamy, L. K. (1998). "Phase transfer catalysis: chemistry and engineering." *AIChE Journal*, 44, 612-646.

Neta P., Madhavan V., Zemel H., Fessenden R. (1977). "Rate constants and mechanism of reaction of sulfate radical anion with aromatic compounds". *J. Am. Chem. Soc.*, 99, 163-164.

Norman, R.O.C., Storey, P.M., and P.R. West. (1970). "Electron spin resonance studies. Part XXV. Reactions of the sulphate radical anion with organic compounds". *J. Chem. Soc. B*, 1087-1095.

Ono, Y., Matsumura, T., Kitajima, N., and Fukuzumi, S.-I. (1977). "Formation of superoxide ion during the decomposition of hydrogen peroxide on supported metals." *J. Phys. Chem.*, 81, 1307-1311.

Roberts, J. L., Calderwood, T. S., and Sawyer, D. T. (1983). "Oxygenation by superoxide ion of CCl_4, $FCCl_3$, $HCCl_3$, p,p'-DDT, and related trichloromethyl substrates ($RCCl_3$) in aprotic solvents." *J. Am. Chem. Soc.*, 105, 7691-7696.

Roberts, J. L., and Sawyer, D. T. (1981). "Facile degradation by superoxide ion of carbon tetrachloride, chloroform, methylene chloride, and p,p'-DDT in aprotic media." *J. Am. Chem. Soc.*,103, 712-714.

Root, D.K., Lay, E.M., Block, P.A., and W.G. Cutler. (2005). "Investigation of chlorinated methanes treatability using activated sodium persulfate". Proceedings of the First International Conference on Environmental Science and Technology, New Orleans, Louisiana.

Sawyer, D. T., and Martell, A. E. (1992). *Industrial environmental chemistry. Waste minimization in industrial processes and remediation of hazardous waste*, Plenum Press, New York.

Sawyer, D. T., and Valentine, J. S. (1981). "How super is the superoxide?" *Acc. Chem. Res.,*14, 393-400.

Siegrist, R. L., Urynowicz, M. A., West, O. R., Crimi, M. L., and Lowe, K. S. (2001). *Principles and practices for in situ chemical oxidation with permanganate*, Battelle Press, Columbus, Ohio.

Singh, P.S., and D.H. Evans. 2006. "Study of the electrochemical reduction of dioxygen in acetonitrile in the presence of weak acids". *J. Phys. Chem. B*, 110, 637-644.

Singh, U. C., and Venkatarao, K. (1976). "Decomposition of peroxodisulphate in aqueous alkaline solution." *J. Inorg. Nucl. Chem.,* 38, 541-543.

Smith, B. A., Teel, A. L., and Watts, R. J. (2004). "Identification of the reactive oxygen species responsible for carbon tetrachloride degradation in modified Fenton's systems." *Environ. Sci. Technol*, 38, 5465-5469.

Sugimoto, H., Matsumoto, S., and Sawyer, D. T. (1987). "Oxygenation of polychloro aromatic hydrocarbons by superoxide ion in aprotic media." *J. Am. Chem. Soc.*, 109, 8081-8082.

Sugimoto, H., Matsumoto, S., and Sawyer, D. T. (1988). "Degradation and dehalogenation of polychlorobiphenyls and halogenated aromatic molecules by superoxide ion and by electrolytic reduction." *Environ. Sci. Technol.*, 22, 1182-1186.

U. S. Environmental Protection Agency (U.S.EPA). (2004). "Cleaning up the nation's waste sites:markets and technology trends." *Office of Solid Waste and Emergency Response* EPA 542-R-04-015.

Walling, C., and R.A. Johnson, (1975). "Fenton's reagent. V. Hydroxylation and side chain cleavage of aromatics". *J. Am. Chem. Soc.*, 97, 363–367.

Watts, R. J. (1998). *Hazardous wastes: sources pathways receptors*, John Wiley & Sons, New York.

Watts, R. J., Bottenberg, B. C., Jensen, M. E., Hess, T. H., and Teel, A. L. (1999). "Mechanism of the enhanced treatment of chloroaliphatic compounds by Fenton-like reactions." *Environ. Sci. Technol.*, 33, 3432-3437.

Watts, R. J., and Teel, A. L. (2006). "Treatment of contaminated soils and groundwater using ISCO." *Practice Periodical of Hazardous, Toxic, and Radioactive Waste Management*, 2-9.

Weber, W. P., and Gokel, G. W. (1977). *Phase transfer catalysis in organic synthesis*, Springer-Verlag, New York.

Zhang, X., and Klabunde, K. J. (1992). "Superoxide on the surface of heat-treated ceria. Intermediates in the reversible oxygen to oxide transformation." *Inorg. Chem.*, 31, 1706-1709.

Zhou, W., Anitescu, G., Rice, P. A., and Tavlarides, L. L. (2004). "Supercritical fluid extraction-oxidation technology to remediate PCB-contaminated soils/sediments: an economic analysis." *Environ. Prog.*, 23, 222-231.

Table 1. Degradation efficiency of ISCO technologies (ITRC Technical and Regulatory Guidance 2007).

Oxidant	Amenable contaminants of concern	Reluctant contaminants of concern	Recalcitrant contaminants of concern	Byproducts
Catalyzed hydrogen peroxide propagations (CHP)	TCA, PCE, TCE, DCE, VC, BTEX, chlorobenzene, phenols, 1,4-dioxane, MTBE, tert-butyl alcohol (TBA), high explosives	DCA, CH_2Cl_2, PAHs, carbon tetrachloride, PCBs	$CHCl_3$, pesticides	Fe(III), O_2, H_2O
Ozone	PCE, TCE, DCE, VC, BTEX, chlorobenzene, phenols, MTBE, TBA, high explosives	DCA, CH_2Cl_2, PAHs	TCA, carbon tetrachloride, $CHCl_3$, PCBs, pesticides	O_2
Permanganate (K/Na)	PCE, TCE, DCE, VC, BTEX, PAHs, phenols, high explosives	Pesticides	Benzene, TCA, carbon tetrachloride, $CHCl_3$, PCBs	Mn (VI)
Activated Sodium Persulfate	PCE, TCE, DCE, VC, BTEX, chlorobenzene, phenols, 1,4-dioxane, MTBE, TBA	PAHs, explosives, pesticides	PCBs	SO_4^{2-}

Table 2. Reaction rate constants between superoxide and hydrocarbons in dimethylformamide (Afanas'ev 1989; Sawyer 1992).

Substrate	$O_2^{-\bullet}$/s	$K_1/[S]$ ($M^{-1}s^{-1}$)
Carbon tetrachloride	5.0	3.8×10^{3}
Trichloromethane	4.0	4×10^{-1}
cis-1,2-Dichloroethene	4.0	1×10^{1}
Hexachloroethane	N/A	4×10^{2}
Hexachlorobenzene	12.0	1×10^{3}
Pentachlorobenzene	11.0	8×10^{1}
1,2,3,4-Tetrachlorobenzene	10.0	2×10^{0}

Table 3. Reaction rate constants between hydroxyl/sulfate radicals and aliphatic and aromatic compounds (Neta 1977).

Substrate	$K_{OH\bullet}$ ($M^{-1}s^{-1}$)	$K_{SO4\bullet-}$ ($M^{-1}s^{-1}$)
Methanol	9.7×10^{8}	1.6×10^{7}
Ethanol	1.9×10^{9}	7.8×10^{7}
2-Propanol	2.0×10^{9}	4.6×10^{7}
tert-Butyl alcohol	5.2×10^{8}	8.9×10^{5}
1-Hexanol	5.2×10^{9}	1.6×10^{8}
Benzene	7.8×10^{9}	3.0×10^{9}
Benzoic acid	4.0×10^{9}	1.2×10^{9}
Anisole	6.0×10^{9}	4.9×10^{9}
Nitrobenzene	3.9×10^{9}	$\leq 10^{6}$

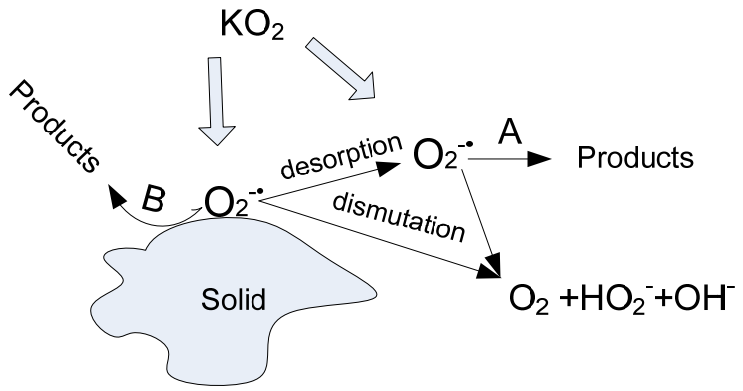

Figure 1. Schematic representation of superoxide reactivity in aqueous heterogeneous environments. A,B: highly oxidized organic compounds.

CHAPTER 2: VOLUME REDUCTION OF NONAQUEOUS MEDIA CONTAMINATED WITH PCDDs ASSOCIATED WITH PESTICIDE WASTE USING SUPEROXIDE

Introduction

Many highly halogenated hydrophobic organic contaminants are a significant threat to human health and the environment. These compounds, which include chlorobenzenes, flame retardants, higher polychlorinated biphenyls (PCBs), and polychlorinated dibenzo-*p*-dioxins (PCDDs), are characterized by minimal free energy, and therefore have a low thermodynamic chemical potential for biotic and abiotic transformations.

PCDDs are commonly found in waste oils, mineral oils, organic sludges, and other nonaqueous environments. For example, waste oils tainted with PCDDs were spread on roads and at horse corrals at Times Beach, Missouri, making it a major Superfund site *(1)*. When trace concentrations of toxic PCDDs are present in much less toxic oils or sludges, the entire system is considered a hazardous waste, and must be managed under the Resource Conservation and Recovery Act (RCRA). One of the most common approaches to pollution prevention is volume reduction. If traces of highly toxic contaminants can be destroyed within a large pool of less toxic oil or sludge, the entire material becomes less hazardous and may no longer be considered a RCRA hazardous waste; it could have another use, such as fuel blending or land application.

The destruction of PCDDs in oils and other nonaqueous media represents a unique challenge. Nearly all species capable of destroying PCDDs are reactive only in water (e.g., bacteria, hydroxyl radical, zero valent iron) *(2)*. However, the transient oxygen species superoxide ($O_2\bullet^-$) is highly reactive with PCDDs in nonaqueous media, though it is unreactive with such contaminants in water *(3)*. Furthermore, because superoxide is a reductant and a nucleophile, it reacts with halogenated contaminants, but not with hydrocarbon-based oils or

sludges *(4)*. Superoxide can be added directly to contaminated nonaqueous media as potassium superoxide along with a phase transfer catalyst (PTC) *(5)*; however, such a process is expensive due to the high cost of potassium superoxide. Less expensive methods involve generating superoxide in water; e.g., through the catalyzed decomposition of peroxygens, such as catalyzed H_2O_2 propagations (CHP—modified Fenton's reagent) *(6)*:

$$H_2O_2 + Fe^{2+} \rightarrow OH\bullet + OH^- + Fe^{3+} \quad (1)$$

$$OH\bullet + H_2O_2 \rightarrow O_2\bullet^- + H_2O + H^+ \quad (2)$$

Superoxide can also be generated in water by electrochemical and photochemical processes *(4, 7-9)*. However, if these more economical methods are used to generate superoxide in water, then the superoxide must be brought into contact with the contaminants in the nonaqueous phase.

The purpose of this research was to investigate the reactivity of superoxide in mixed aqueous–nonaqueous systems as a basis for the volume reduction of PCDD-contaminated oils and sludges using the organic solvents acetone and dimethyl sulfoxide (DMSO) as models for nonaqueous systems. The use of aqueous superoxide solutions is necessary for economical superoxide treatment of contaminated oils and sludges, but the presence of water may decrease superoxide reactivity; therefore, the effect of adding water to superoxide– nonaqueous systems was first evaluated. If sufficient superoxide reactivity can be retained with representative addition of water (e.g., up to 10% water [v/v]), then such an approach may be viable. The second segment of this research focused on superoxide reactivity in the same two solvent systems as a basis for destroying PCDDs by promoting the phase transfer of superoxide from the aqueous phase into the organic phase.

Materials and Methods

Materials

Potassium superoxide (KO_2, 96.5 %), polyethylene glycol-400 (PEG), and 18-crown-6-ether (99%) were purchased from Alfa Aesar (Ward Hill, MA) and used without modification. Hexachlorobenzene (HCB, 99%) and diethylenetriamine pentaacetic acid (DTPA, 97%) were purchased from Sigma-Aldrich (St. Louis, MO). Toluene (99.9%), acetone (99.7%), DMSO, (99.9%), potassium hydroxide (87.9%), and sodium hydroxide (99.3%) were J.T. Baker products (Phillipsburg, NJ). Double-deionized water was purified to > 18 MΩ•cm using a Barnstead E-pure system.

Sodium hydroxide solutions were purified to remove transition metals by the addition of magnesium hydroxide *(10, 11)*. The magnesium hydroxide-NaOH solution was stirred for 8 hr, the floc that formed was allowed to settle, and the solution was passed through a 0.45 μm filter to remove the residual floc.

Probe compound

Hexachlorobenzene (HCB) was used as a probe compound for reactions with superoxide (k_{O2}•- =1 x 10^3 $M^{-1}sec^{-1}$ in dimethylformamide *(12-14)*; HCB has been used as a surrogate for 2,3,7,8-tetrachlorodibenzo-*p*-dioxin in environmental chemodynamic studies *(15)*, because it is similarly hydrophobic and biorefractory, but is significantly less toxic.

Effect of water on superoxide reactivity in model nonaqueous phases

The solvents acetone and DMSO were used as model nonaqueous phases because they represent organic solvents that are miscible with water, and thus have high potential for the addition of water to lower superoxide reactivity. Therefore, if superoxide reactivity can be maintained in these solvents when water is added, then even greater superoxide reactivity could

be achieved in more hydrophobic oil-based systems in the presence of water. In addition, acetone and DMSO form separate nonaqueous phases when aqueous KO_2 is added, so that the phase transfer of superoxide from the aqueous to the nonaqueous phase could be then be evaluated using the same model solvents.

KO_2 was dissolved in acetone and DMSO by suspending KO_2 powder in each of the solvents followed by addition of 18-Crown-6-ether *(16)*. The solution was mixed for 10 min; the remaining solid KO_2 was allowed to settle, and the liquid phase was decanted into reaction vessels, which were 20 ml borosilicate volatile organic analysis (VOA) vials capped with PTFE-lined septa. Hexachlorobenzene was then added to the solution followed by the addition of varying volumes of water. The total reaction volume was 20 ml and consisted of 75 mM crown ether, 30 mM KO_2, and 0.02 mM HCB, with a range of water concentrations: 0–15% (v/v) for the acetone reactions, and 0–25% for the DMSO reactions. A set of reaction vials was quenched at 1 min intervals by adding 8 ml of water, which was then extracted with 5 ml of toluene. The extracts were then analyzed for residual HCB by gas chromatography. All reactions were conducted in triplicate at 20 ± 2 ˚C, and triplicate control reactors were established in parallel without the addition of KO_2.

Superoxide reactivity in water–solvent two-phase systems

Two-phase reactions were conducted in triplicate 20 mL borosilicate VOA vial reactors. The two phases consisted of an aqueous phase of 5 ml of 3 M KO_2, 33 mM purified NaOH, and 1 mM DTPA (to inactivate transition metals), and a nonaqueous phase of 9 ml of organic solvent (acetone or DMSO, for a solvent proportion of 60% v/v) spiked with 0.02 mM HCB. Upon addition of the organic solvent, separation of the two phases was instantaneous due to the salting effect of the KO_2. Phase transfer catalysts (PTCs) were added to a final concentration of 0.15 M

and a final reaction volume of 15 ml. Control reactors contained additional solvent in place of the PTC; in addition, control reactors for the DMSO systems contained additional DMSO in place of the KO_2, because the KO_2 –DMSO system resulted in HCB degradation even in the absence of PTCs. At selected time points, the total reactor contents were extracted with 20 ml of toluene and analyzed for HCB by gas chromatography.

The same procedure was repeated using 3 M KOH as a salting agent in place of KO_2. These reactions were run to differentiate the effect of KO_2 on HCB degradation in the organic phase from any effect that might be due to the KOH, because KO_2 in water generates KOH during disproportionation *(4, 17)*.

Analysis

Toluene extracts were analyzed for HCB using a Hewlett-Packard 5890 gas chromatograph with a 0.53 mm (i.d.) × 60 m Equity 1 capillary column and electron capture detector (ECD). The injector temperature was 300 ˚C, the detector temperature was 325 ˚C, the initial oven temperature was 60 ˚C, the program rate was 30 ˚C min^{-1}, and the final temperature was 300 ˚C.

Results and discussion

Effect of water on superoxide reactivity in acetone and DMSO

Increasing volumes of deionized water were added to two organic solvent systems containing superoxide, and relative superoxide reactivity was measured using the probe compound HCB. These experiments provided fundamental information about potential superoxide reactivity in PCDD-containing nonaqueous phases when water is added as part of a superoxide–water solution. The effect of water addition on superoxide reactivity in crown ether–

KO_2–acetone systems is shown in Figure 1. The superoxide probe HCB degraded 98% in 3 min in the crown ether–KO_2–acetone system; however, HCB degradation rates decreased with increasing water concentrations. The presence of 2.5% (v/v) water in the system lowered the reactivity of superoxide, resulting in 30% HCB degradation after 5 min. In systems containing 10% and 15% water, HCB degradation was 12% after 5 min relative to the control system. The effect of adding water on the relative reactivity of superoxide in crown ether–KO_2–DMSO systems is shown in Figure 2. The superoxide probe HCB degraded by 98% over 30 sec in the crown ether–KO_2–DMSO system. As in the acetone systems, HCB degradation rates decreased with increasing water concentrations. The presence of 5% and 10% water in the DMSO systems lowered the reactivity of superoxide, resulting in 62% and 31% HCB degradation, respectively, after 30 sec. In systems containing 15%, 20%, and 25% water, HCB degradation after 5 min was 90%, 40%, and 15%, respectively.

The results of Figures 1 and 2 confirm that superoxide has different characteristics in the presence of water vs. in pure organic media such as acetone or DMSO. In organic media, superoxide is long-lived *(4)* due to its solvation state, and its longevity makes it highly reactive. When superoxide is solvated by an organic molecule such as acetone, the electromotive force for a one-electron transfer (E^o) ($O_2/O_2\bullet^-$) is –0.88 V, making superoxide highly reactive with a wide range of organic compounds including PCDDs *(18)*. In contrast, four water molecules solvate superoxide in aqueous systems; because of the change in its solvation state, superoxide has an E^o ($O_2/O_2\bullet^-$) of –0.19 V, and is short-lived (half-life <1 sec) because it undergoes rapid disproportionation *(4, 17-21)*:

$$2O_2\bullet^- + H_2O \rightarrow HO_2^- + OH^- + O_2 \qquad (3)$$

As water was added to the acetone and DMSO systems (Figures 1 and 2), the superoxide solvation shells that were originally filled with the organic solvent were likely partially replaced with water, resulting in a shorter lifetime and lower reactivity with HCB.

While addition of water to superoxide systems lowered the reactivity of superoxide, a measurable degree of superoxide reactivity remained with water contents up to 15% in acetone and 25% in DMSO. Therefore, water-based superoxide generation will not likely negate superoxide reactivity in the treatment of contaminated oils and sludges. Economical approaches to generating superoxide, such as the MnO_2-catalyzed decomposition of hydrogen peroxide *(22)*, would inherently add water to the nonaqueous system that is being treated (e.g., a drum of waste oil tainted with PCDDs). The results of Figures 1 and 2 demonstrate that although adding small amounts of MnO_2-hydrogen peroxide in water to a contaminated nonaqueous phase would slow the reaction rate of superoxide with the contaminant, the process could still provide effective treatment.

Superoxide reactivity in heterogeneous organic solvent–water systems

The second phase of this research focused on promoting the phase transfer of superoxide generated in the aqueous phase to nonaqueous phase oils and sludges. In order to compare the results of the two parts of the study, the same two solvents, acetone and DMSO, were used. Although acetone and DMSO are miscible in water, near-complete phase separation of water–acetone and water–DMSO systems containing >10% (v/v) water was accomplished by adding 3 M aqueous KO_2 (Figure 3a). KO_2 behaved as a salting agent in organic solvent–water mixtures and promoted phase separation between water and the organic solvent *(23)*. To confirm that the phase separation was due to a salting effect, the procedures were repeated using KOH in place of KO_2 (Figure 3b). Equal volumes of the organic phases separated in both water–KO_2–acetone and

water–KOH–acetone systems. In both acetone and DMSO systems, > 99% of the organic solvent was recovered as a phase separate from the water. These results demonstrate that acetone and DMSO could be used to create two-phase water–organic solvent systems that could be directly compared to the systems used in Figures 1 and 2.

Using these two-phase systems, the potential for superoxide added to the aqueous phase to migrate to the organic solvent phase was evaluated as a basis for the treatment of PCDDs in nonaqueous organic phases. When added to these systems, the superoxide probe HCB immediately partitioned into the organic phase. The degradation of HCB in the organic phase of water–KO_2–acetone and water–KO_2–DMSO systems when superoxide was added to the aqueous phase is shown in Figure 4a-b. No measurable degradation of HCB occurred in the two-phase water–KO_2–acetone system; however, 73% HCB degradation occurred within 12.5 min in the two-phase water–KO_2–DMSO system. The results of Figure 4 suggest that superoxide did not diffuse through the interface of the two-phase water–acetone system, but did cross the water–DMSO phase boundary in the water–DMSO system. Acetone is less polar than DMSO and may have higher interfacial tension when in contact with water, which may minimize superoxide transfer from the aqueous phase into acetone *(5)*.

The interface formed between two distinct liquid phases often limits reactivity in the organic phase if the reactive species is generated in the aqueous phase; therefore, phase transfer catalysts (PTCs) are often used to enhance the transfer of a nucleophile from the aqueous phase into the organic phase *(5, 24-26)*.

The PTCs 18-Crown-6 ether and PEG were compared for their abilities to transfer superoxide from the aqueous phase into the overlying organic phase in two-phase water–KO_2–acetone and water–KO_2–DMSO systems. PEG was chosen as a PTC because it complexes K^+ in

a manner similar to crown ethers *(27,28)*, but is less expensive and more environmentally benign *(29)*; the crown ether served as a benchmark PTC because it has been used extensively in previous studies *(5, 26)*. The loss of HCB in two-phase water–crown ether–KO_2–acetone systems and water–PEG–KO_2–acetone systems is shown in Figure 5. The superoxide probe HCB degraded 63% over 45 min in the acetone phase using both the PEG and the crown ether. These data demonstrate that both PTCs promoted a similar increase in superoxide activity in acetone compared to KO_2 alone by promoting the transfer of the superoxide from the aqueous phase to the organic phase.

The effect of PTCs on superoxide activity in the two-phase water–KO_2–DMSO systems is shown in Figure 6. The presence of both the crown ether and the PEG significantly increased degradation of the superoxide probe HCB in both of the two-phase water–PTC–KO_2–DMSO systems, compared to the control systems in which no PTC was added. Addition of the crown ether or the PEG resulted in 97% or 96% HCB degradation, respectively, over 12.5 minutes in the water–PTC–KO_2–DMSO systems.

The results shown in Figures 5 and 6 demonstrate that the two PTCs improved the transport of superoxide across the phase boundary in both of the two-phase water–KO_2–organic solvent systems, allowing superoxide to react with HCB in the organic phase. Furthermore, PEG proved to be approximately as effective as the crown ether in these systems. These results also confirm that the minimal superoxide activity in the two-phase systems shown in Figure 4 was due to a negligible mass of superoxide crossing the phase boundary.

To evaluate whether other reaction pathways in the water–PTC–KO_2–organic solvent systems are occurring, the experiments were repeated with the use of KOH in place of KO_2. A possible reaction pathway in the water–PTC–KO_2–solvent systems is the decomposition of KO_2

to KOH in the aqueous phase (equation 3), phase transfer of KOH into the organic phase, and nucleophilic attack by hydroxide. HCB degradation in water–PTC–KOH–acetone systems is shown in Figure 7. HCB degraded 16% over 60 min in the two-phase water–PEG–KOH–acetone system; however, there was no significant HCB degradation in the two-phase water–crown–KOH–acetone system. These results suggest that hydroxide does not directly attack HCB in the organic phase. A possible pathway of HCB degradation in the two-phase water–PEG– KOH–acetone system is a nucleophilic attack by $PEGO^-$ (PEG in the presence of NaOH) *(27, 28, 30)*. $PEGO^-$ could be partially responsible for HCB degradation in the parallel systems containing PEG and superoxide (Figure 5). However, the 62% HCB degradation in the acetone phase of the water–PEG–KO_2–acetone systems was significantly higher than in the water–PEG–KOH–acetone systems, which indicates that superoxide is responsible for the majority of the HCB degradation in the two-phase water–PEG–KO_2–acetone systems. In contrast, there was no significant degradation of HCB in the two-phase water–crown ether–KOH–acetone systems (Figure 7).

HCB degradation in the two-phase water–PTC–KOH–DMSO systems is shown in Figure 8. Both of the two-phase systems behaved similarly to the parallel acetone systems (Figure 7). HCB degradation was 39% over 12.5 min in the two-phase water–PEG–KOH–DMSO systems; these results suggest that $PEGO^-$ degraded HCB, similar to the degradation that occurred in the parallel acetone system. However, degradation of HCB was significantly more rapid in the parallel system containing superoxide (Figure 6). In the two-phase water–crown ether–KOH–DMSO system, minimal HCB degradation occurred. The results of Figures 5–8 demonstrate that superoxide was the predominant reactive species in the degradation of HCB in the two-phase water–organic solvent systems studied.

The results of the first part of this research demonstrate that superoxide reactivity in model nonaqueous systems was reduced by the addition of water, but sufficient reactivity was maintained to achieve destruction of the PCDD surrogate HCB. In the second segment of the research, superoxide was generated in the aqueous phase of two-phase water–organic solvent systems, and there was minimal flux of superoxide across the phase boundary into the organic solvent. However, when a PTC was added to the system, superoxide transfer from the aqueous phase resulted in reactivity and HCB destruction in the nonaqueous phase. Superoxide can be generated in water electrochemically, photochemically, or through the metal oxide-catalyzed decomposition of hydrogen peroxide. If PTCs are used in conjunction with superoxide generation in the aqueous phase, hydrophobic contaminants such as PCDDs in oils, sludges, and other contaminated nonaqueous media may potentially be destroyed by superoxide–PTC treatments, providing volume reduction of the contaminated media. Furthermore, the environmentally benign PTC PEG was as effective as the crown ether in promoting superoxide phase transfer across the water–organic solvent phase boundary. The results of this research provide proof of concept of the use of aqueous superoxide to destroy hydrophobic organic contaminants in nonaqueous media. Subsequent studies will focus on volume reduction of oils and sludges contaminated with hydrophobic organic contaminants using economical water-based processes to generate superoxide, such as the catalyzed decomposition of peroxygens.

When trace quantities of toxic polychlorinated organic compounds contaminate otherwise nonhazardous waste oils, mineral oils, and oily sludges, the entire system is classified as a hazardous waste. A common practice in pollution prevention is volume reduction; i.e., destroying traces of toxic contaminants in a large volume of material so that it is no longer hazardous. The potential for using superoxide to treat polychlorinated organic compounds, such

as PCDDs, in nonaqueous media was investigated. Although superoxide is unreactive with polychlorinated organic compounds in water, its reactivity was still significant enough to degrade the PCDD surrogate HCB when water was added to the solvents acetone and DMSO. Therefore, superoxide generated in an aqueous phase mixed with a hydrocarbon-based organic waste containing trace concentrations of PCDDs could still be effective in destroying the contaminant. Superoxide generated in the aqueous phase does not cross the phase boundary and enter the nonaqueous phase. However, the PTC PEG-400 effectively promoted the transfer of superoxide from water into a separate organic phase as efficiently as the more expensive PTC 18-Crown-6 ether. The results of this study show that superoxide, which can be economically generated in water, has the potential to destroy trace concentrations of polychlorinated organic contaminants in nonaqueous phase systems, such as hydrocarbon-based oils and sludges. Such a process could potentially render the nonaqueous phase nonhazardous, allowing it to be used for fuel blending or other beneficial purposes.

Acknowledgements

Funding for this research was provided by the Strategic Environmental Research and Development Program (SERDP) through Grant No. CU-1288.

Literature Cited

(1) Watts, R. J. *Hazardous wastes: sources pathways receptors*. John Wiley & Sons: New York, 1998.

(2) Larson, R. A.; Weber, E. J. *Reaction mechanisms in environmental organic chemistry*. Lewis Publishers: New York, 1994.

(3) Halliwell, B.; Gutteridge, J. M. C. *Free radicals in biology and medicine*. Clarendon Press: Oxford, 1985.

(4) Afanas'ev, I. B. *Superoxide ion: chemistry and biological implication*. CRC Press, Inc: Boca Raton, 1989; Vol. 1, p 279.

(5) Weber, W. P.; Gokel, G. W. *Phase transfer catalysis in organic synthesis*. Springer-Verlag: New York, 1977.

(6) Watts, R. J.; Teel, A. L. Chemistry of modified Fenton's reagent (catalyzed H_2O_2 propagations-CHP) for in situ soil and groundwater remediation. *J. Environ. Eng.* **2005,** 131, 612-622.

(7) Ono, Y.; Matsumura, T.; Kitajima, N.; Fukuzumi, S.-I. Formation of superoxide ion during the decomposition of hydrogen peroxide on supported metals. *J. Phys. Chem.* **1977,** 81, 1307-1311.

(8) Anpo, M.; Che, M.; Fubini, B.; Garrone, E.; Giamello, E.; Paganini, M. C. Generation of superoxide ions at oxide surfaces. *Top. Catal.* **1999,** 8, 189-198.

(9) Sawyer, D. T.; Martell, A. E. *Industrial environmental chemistry. Waste minimization in industrial processes and remediation of hazardous waste*. Plenum Press: New York, 1992.

(10) Monig, J.; Bahnemann, D.; Asmus, K.-D. One electron reduction of CCl_4 in oxygenated aqueous solutions: a CCl_3O_2-free radical mediated formation of Cl^- and CO_2. *Chem. Biol. Interact.* **1983,** 47, 15-27.

(11) Smith, B. A.; Teel, A. L.; Watts, R. J. Identification of the reactive oxygen species responsible for carbon tetrachloride degradation in modified Fenton's systems. *Environ. Sci. Technol.* **2004,** 38, 5465-5469.

(12) Lee, J. L.; Yao, C. P.; Wang, Y. Y.; Wan, C. C. Electrochemical decomposition of chlorinated benzenes in dimethylformamide solvent. *Environ. Sci. Technol.* **1992,** 26, 553-556.

(13) Sugimoto, H.; Matsumoto, S.; Sawyer, D. T. Oxygenation of polychloro aromatic hydrocarbons by superoxide ion in aprotic media. *J. Am. Chem. Soc.* **1987,** 109, 8081-8082.

(14) Sugimoto, H.; Matsumoto, S.; Sawyer, D. T. Degradation and dehalogenation of

polychlorobiphenyls and halogenated aromatic molecules by superoxide ion and by electrolytic reduction. *Environ. Sci. Technol.* **1988,** 22, 1182-1186.

(15) Arthur, M. F.; Frea, J. I. Microbial activity in soils contaminated with 2,3,7,8-TCDD. *Environ. Toxicol. Chem.* **1988,** 7, 5-13.

(16) Niehaus, W. G. A proposed role of superoxide anion as a biological nucleophile in the deesterification of phospholipids. *Bioorg. Chem.* **1978,** 7, 77-84.

(17) Bielski, B. H. J.; Allen, O. Mechanisms of the disproportionation of superoxide radicals. *J. Phys. Chem.* **1977,** 81, 1048-1050.

(18) Roberts, J. L.; Calderwood, T. S.; Sawyer, D. T. Oxygenation by superoxide ion of CCl_4, $FCCl_3$, $HCCl_3$, p,p'-DDT, and related trichloromethyl substrates ($RCCl_3$) in aprotic solvents. *J. Am. Chem. Soc.* **1983,** 105, 7691-7696.

(19) Andrieux, C. P.; Hapiot, P.; Saveant, J.-M. Mechanism of superoxide ion disproportionation in aprotic solvents. *J. Am. Chem. Soc.* **1987,** 109, 3768-3775.

(20) Che, Y.; Tsushima, M.; Matsumato, F.; Okajima, T.; Tokuda, K.; Ohsaka, T. Water-induced disproportionation of superoxide ion in aprotic solvents. *J. Phys. Chem.* **1996,** 100, 20134-20137.

(21) Chin, D.-H.; Chiericato, G.; Nanni, E. J.; Sawyer, D. T. Proton-induced disproportionation of superoxide ion in aprotic media. *J. Am. Chem. Soc.* **1982,** 104, 1296-1299.

(22) Furman, O.; Laine, D. F.; Blumenfeld, A.; Teel, A. L.; Shimizu, K.; Cheng, I. F.; Watts, R. J. Enhanced reactivity of superoxide in water-solid matrices. *Environ. Sci. Technol.* **2009,** 43, 1528-1533.

(23) Matkovich, C. E.; Christian, G. D. Salting-out of acetone from water-basis of a new solvent extraction system. *Anal. Chem.* **1973,** 45, 1915-1921.

(24) Herriott, A. W.; Picker, D. Phase transfer catalysis. An evaluation of catalysis. *J. Am. Chem. Soc.* **1975,** 97, 2345-2349.

(25) Naik, S. D.; Doraiswamy, L. K. Phase transfer catalysis: chemistry and engineering. *AIChE Journal* **1998,** 44, 612-646.

(26) Starks, C. M. Modern perspectives on the mechanisms of phase-transfer catalysis. In *Phase-transfer catalysis mechanisms*, Halpern, M. E., Ed. ACS: Washington, DC, 1997.

(27) Brunelle, D. J.; Mendiratta, A. K.; Singleton, D. A. Reaction/removal of polychlorinated biphenyls from transformer oil: treatment of contaminated oil with poly(ethylene glycol)/KOH. *Environ. Sci. Technol.* **1985,** 19, 740-746.

(28) Brunelle, D. J.; Singleton, D. A. Destruction/removal of polychlorinated biphenyls from non-polar media. Reaction of PCB with Poly(ethylene glycol)/KOH. *Chemosphere* **1983,** 12, 183-186.

(29) Chen, J.; Spear, S. K.; Huddleston, J. G.; Rogers, R. D. Polyethylene glycol and solutions of polyethylene glycol as green reaction media. *Green Chem.* **2005,** 7, 64-82.

(30) Pytlewski, L. L.; Krevitz, K.; Smith, A. B. Composition for decomposing halogenated organic compounds. U. S. Patent 4471143, 1982.

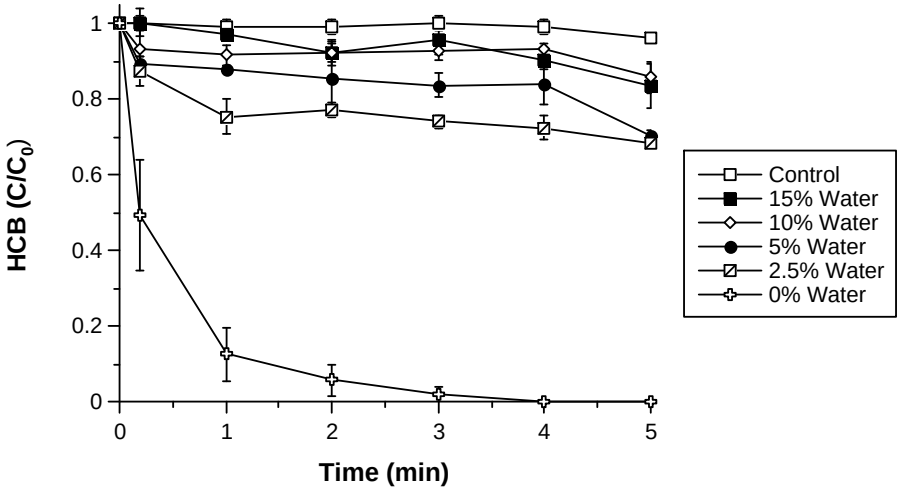

Figure 1. Effect of water addition on superoxide reactivity in acetone/crown ether/KO_2 systems (reaction conditions: 75 mM crown ether, 30 mM KO_2, and 0.02 mM HCB in acetone containing 0% to 15% deionized water). Error bars represent the standard error of the mean of three replicates.

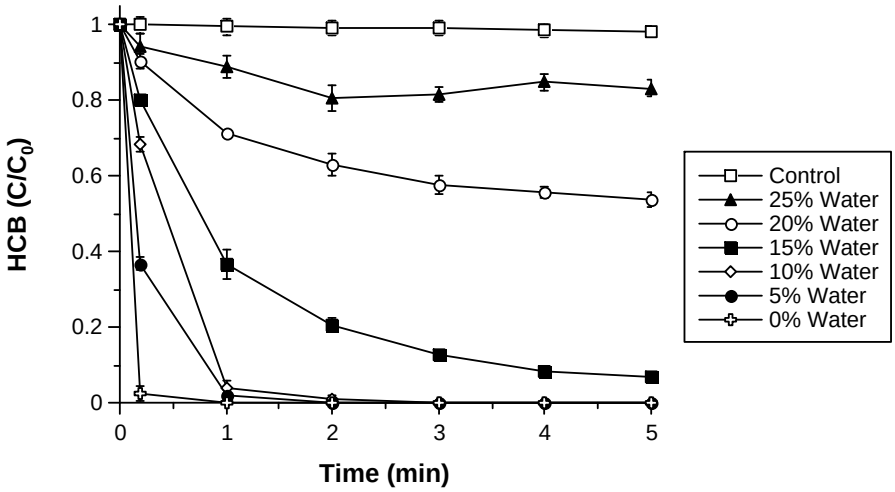

Figure 2. Effect of water addition on superoxide reactivity in DMSO/crown ether/KO_2 systems (reaction conditions: 75 mM crown ether, 30mM KO_2, and 0.02 mM HCB in DMSO containing 0% to 25% deionized water). Error bars represent the standard error of the mean of three replicates.

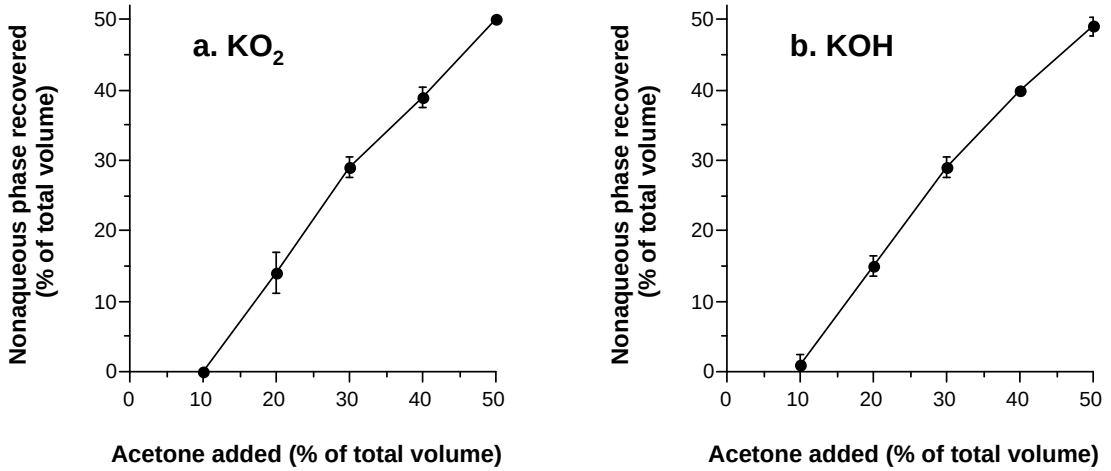

Figure 3. Separation of the acetone phase as a function of the initial acetone volume in acetone/water systems containing a) 3 M KO2, or b) 3 M KOH (reaction conditions: 25 mL of 3 M KO_2 or 3 M KOH added to 25 mL of acetone/water mixtures containing 20% to 100% acetone [v/v].)

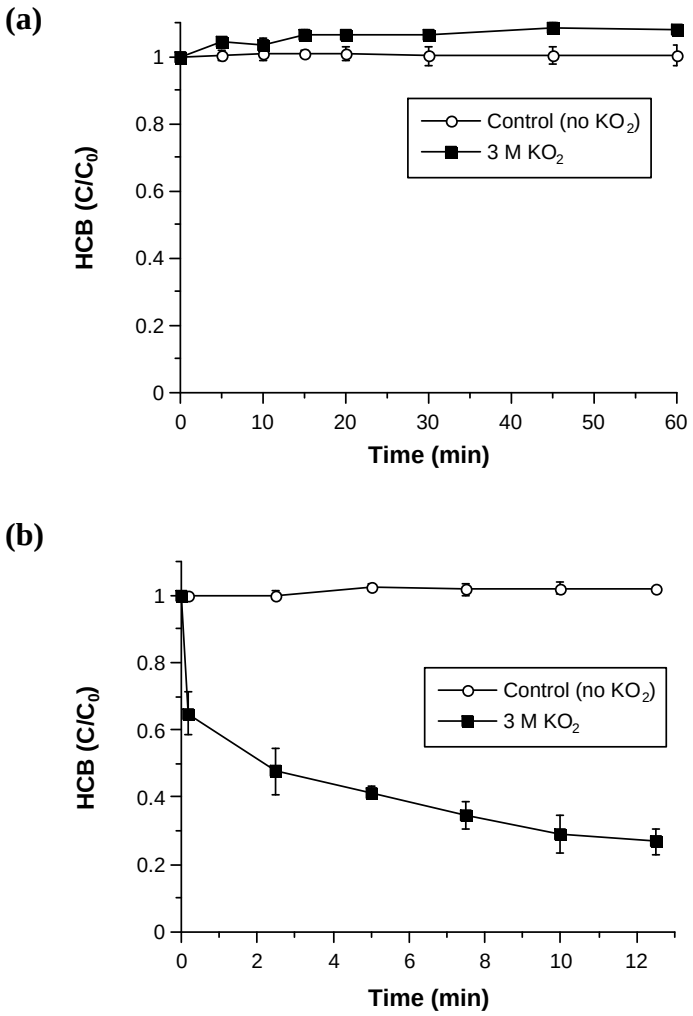

Figure 4. Superoxide reactivity in the organic phase of two-phase systems with 3 M KO_2 added to the aqueous phase of systems containing a) acetone or b) DMSO (reaction conditions: the 5 ml aqueous phase consisted of 3 M KO_2, 33 mM NaOH, and 1 mM DTPA; the 10 ml organic phase consisted of acetone or DMSO containing 0.02 mM HCB). Error bars represent the standard error of the mean of three replicates.

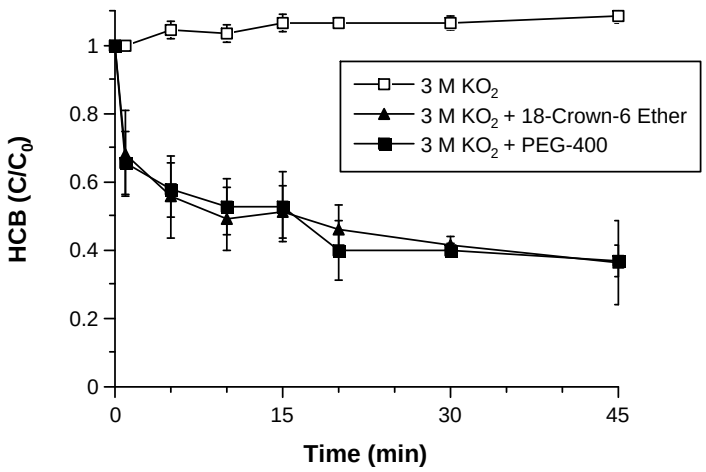

Figure 5. Superoxide reactivity in the organic phase of aqueous KO_2–acetone systems containing the phase transfer catalyst 18-Crown-6 ether and PEG (reaction conditions: the 5 ml aqueous phase contained 3 M KO_2, 33 mM NaOH, and 1 mM DTPA; the 9 ml acetone phase contained 0.02 mM HCB; 0.9 ml of 0.15 M crown ether or 0.15 M PEG was then added for a final volume of 15 ml in the reactors; control reactors contained additional acetone in place of the phase transfer catalyst). Error bars represent the standard error of the mean of three replicates.

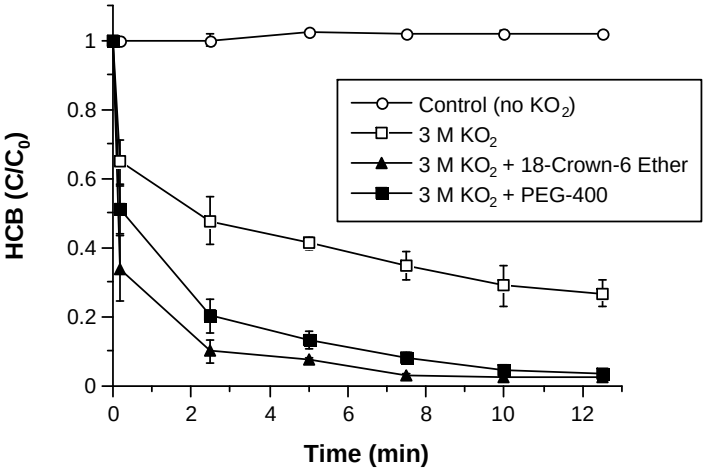

Figure 6. Superoxide reactivity in the organic phase of aqueous KO_2–DMSO systems containing the phase transfer catalyst 18-Crown-6 ether and PEG (reaction conditions: the 5 ml aqueous phase contained 3 M KO_2, 33 mM NaOH, and 1 mM DTPA; the 9 ml DMSO phase contained 0.02 mM HCB; 0.9 ml of 0.15 M crown ether or 0.15 M PEG was then added for a final volume of 15 ml in the reactors; control reactors contained additional DMSO in place of the phase transfer catalyst and in place of the KO_2). Error bars represent the standard error of the mean of three replicates.

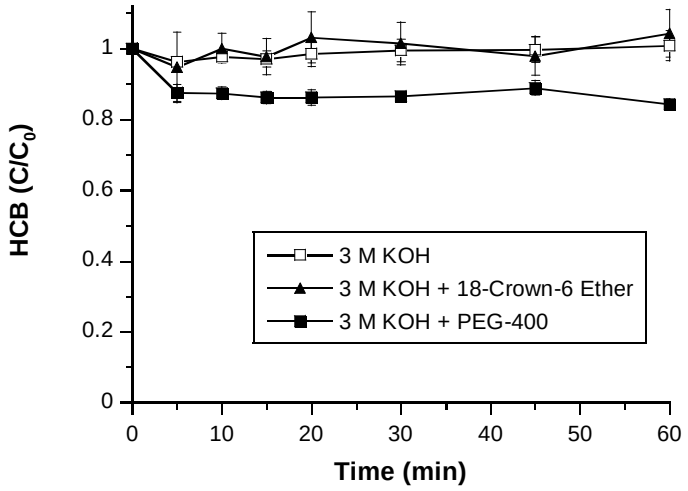

Figure 7. Superoxide reactivity in the organic phase of aqueous KOH–acetone systems containing the phase transfer catalyst 18-Crown-6 ether and PEG (reaction conditions: the 5 ml aqueous phase contained 3 M KOH, 33 mM NaOH, and 1 mM DTPA; the 9 ml acetone phase contained 0.02 mM HCB; 0.9 ml of 0.15 M crown ether or 0.15 M PEG was then added for a final volume of 15 ml in the reactors; control reactors contained additional acetone in place of the phase transfer catalyst). Error bars represent the standard error of the mean of three replicates.

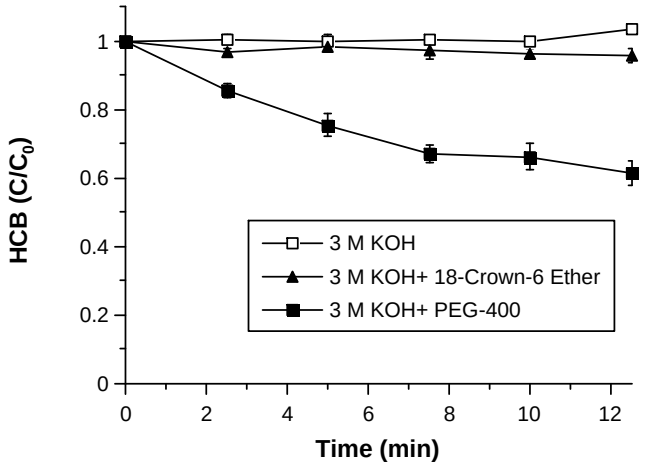

Figure 8. Superoxide reactivity in the organic phase of aqueous KOH–DMSO systems containing the phase transfer catalyst 18-Crown-6 ether and PEG (reaction conditions: the 5 ml aqueous phase contained 3 M KOH, 33 mM NaOH, and 1 mM DTPA; the 9 ml DMSO phase contained 0.02 mM HCB; 0.9 ml of 0.15 M crown ether or 0.15 M PEG was then added for a final volume of 15 ml in the reactors; control reactors contained additional DMSO in place of the phase transfer catalyst). Error bars represent the standard error of the mean of three replicates.

CHAPTER 3: ENHANCED REACTIVITY OF SUPEROXIDE IN WATER-SOLID MATRICES

Introduction

In situ chemical oxidation (ISCO) technologies have become increasingly popular for the remediation of contaminated soils and groundwater. A commonly used ISCO process is catalyzed H_2O_2 propagations (CHP), which is an extension of Fenton's reagent. In the traditional Fenton's process, dilute hydrogen peroxide is added to a degassed solution of iron (II) to provide near stoichiometric generation of hydroxyl radical:

$$H_2O_2 + Fe^{2+} \rightarrow OH^{\bullet} + OH^{-} + Fe^{3+} \quad (1)$$

In CHP systems, the catalyzed decomposition of high concentrations of hydrogen peroxide in the presence of soluble transition metals or minerals results in additional propagation reactions that generate superoxide ($O_2^{\bullet-}$) and hydroperoxide (HO_2^{-}) in addition to hydroxyl radical (*1-4*).

$$OH^{\bullet} + H_2O_2 \rightarrow HO_2^{\bullet} + H_2O \quad (2)$$

$$H_2O_2 + Fe^{3+} \rightarrow HO_2^{\bullet} + Fe^{2+} + H^{+} \quad (3)$$

$$HO_2^{\bullet} \leftrightarrow O_2^{\bullet-} + H^{+} \qquad pK_a = 4.8 \quad (4)$$

$$HO_2^{\bullet} + Fe^{2+} + H^{+} \rightarrow H_2O_2 + Fe^{3+} \quad (5)$$

$$H_2O_2 \leftrightarrow HO_2^{-} + H^{+} \qquad pK_a = 11.8 \quad (6)$$

The application of CHP to the treatment of soils and groundwater has been effective in the degradation of highly oxidized contaminants, such as carbon tetrachloride, hexachloroethane, and chloroform (*2, 4, 5*), that are not destroyed by traditional Fenton's reagent. Recent studies have shown that superoxide is likely the species responsible for such degradation (*1, 6*). Superoxide is a relatively stable radical and a strong nucleophile in aprotic solvents (*7, 8*) but is considered essentially unreactive toward oxidized organic compounds in deionized water, because it forms hydrogen bonds and undergoes rapid disproportionation at all but highly basic

pH regimes (*7, 9–11*). However, Smith et al. (*1*) studied the reactivity of superoxide in aqueous potassium superoxide (KO_2) systems, and found that when H_2O_2 was added to the KO_2 reactions at concentrations similar to those used in CHP systems, superoxide reactivity increased significantly. They obtained similar results when 1 M concentrations of other solvents less polar than water, such as acetone and ethylene glycol, were added to aqueous KO_2 reactions or to CHP reactions as cosolvents, and found that superoxide reactivity correlated strongly with the empirical solvent polarity of the solvents added. Their results indicated that even dilute concentrations of solvents, including H_2O_2, can increase the reactivity of superoxide in water, possibly by altering its solvation shell. In most CHP systems, H_2O_2 concentrations > 0.3 M (1%) are required to provide conditions that increase the reactivity of superoxide sufficiently to degrade carbon tetrachloride and similar oxidized compounds (*1*).However, recent results have demonstrated that such high hydrogen peroxide concentrations are not needed in manganese oxide-catalyzed CHP systems in order to degrade highly oxidized chlorinated compounds. For example, Watts et al. (*3*) demonstrated that the manganese oxide-catalyzed decomposition of low hydrogen peroxide concentrations at near neutral pH generates a species capable of degrading carbon tetrachloride. In contrast, CHP reactions catalyzed by other metal oxides common in the subsurface, such as goethite, ferrihydrite, and hematite, do not degrade carbon tetrachloride (*4*).

The generation of superoxide has been documented in metal oxide–H_2O_2 systems (*12–15*), and it is likely the species responsible for the degradation of carbon tetrachloride in manganese oxide–H_2O_2 CHP systems. However, it is unclear why superoxide should be reactive in a system with a H_2O_2 concentration too low to provide a solvent effect. Manganese oxides are characterized by high surface areas (>50 m^2/g), and we hypothesize that the interaction of surfaces with superoxide may increase superoxide activity, similar to the effect of solvents.

Therefore, the objective of this study was to determine the effect of solid surfaces on superoxide reactivity in aqueous environments.

Experimental Section

Materials. Hexachloroethane (HCA) (99%), 5,5-dimethyl-1-pyrroline-N-oxide (DMPO) (97%), diethylenetriamine-pentaacetic acid (DTPA) (97%) and 1-hexanol (>98%) were purchased from Sigma-Aldrich (St. Louis, MO). Stock solutions of 11 mg/L HCA were prepared prior to conducting reactions and were used within one day. The impurities in DMPO were removed with charcoal followed by filtration until no extraneous electron spin resonance spectroscopy (ESR) signals were observed (*16*). Potassium permanganate, hydrochloric acid, magnesium chloride (99.6%), hydrogen peroxide (50%), and sodium hydroxide (98%) were obtained from J.T. Baker (Phillipsburg, NJ). Mixed hexanes (60%) were purchased from Fisher Scientific (Fair Lawn, NJ). Potassium superoxide (KO_2, 96.5%) was obtained from Alfa Aesar (Ward Hill, MA). Soda-lime glass spheres of varying sizes were purchased from MO-SCI Specialty Products, L.L.C. (Rolla, MO). Double-deionized water was purified to >18 MΩ•cm using a Barnstead E-pure system. Manganese oxide (birnessite, γ-MnO_2) was synthesized according to the procedure described by McKenzie (*17*) by the reduction of boiling $KMnO_4$ with concentrated HCl. The precipitate was vacuum filtered, washed with deionized water to remove salts, and oven dried at 50º C. The structure of birnessite was confirmed by X-ray diffraction, and its surface area was 50.6 m^2/g as measured by BET analysis (*18*).

Detection of Superoxide in MnO_2–H_2O_2 Suspensions Using ESR Spectroscopy. Superoxide was detected with ESR spectroscopy using DMPO as a spin trap agent. The reaction mixture for ESR spin trapping contained a volume of 2.5 mL of 0.2 M H_2O_2 with 1 mg MnO_2. The reactants were mixed with 0.18 M DMPO 1 min after the reaction was initiated, and

immediately injected into an aqueous sample cell (Bruker, AquaX high sensitivity). All spectra were obtained using a Bruker 6/1 spectrometer under the following conditions: resonance frequency, 9.86 GHz; microwave power, 2.0 mW; modulation frequency, 100 kHz; modulation amplitude, 1.0 G; sweep width, 100 G; time constant, 164 ms; sweep time, 168 s; and receiver gain, 2.0×10^5.

General Reaction Conditions. Hydrogen peroxide and potassium superoxide were used as sources of superoxide, and catalytic and noncatalytic solid surfaces were used to generate and/or stabilize superoxide in three reaction systems: 1) H_2O_2–MnO_2, 2) KO_2–MnO_2, and 3) KO_2–inert glass spheres. Hexachloroethane was used as a superoxide probe (k_{O2}•- = 400 $M^{-1}s^{-1}$) (*7*), and 1-hexanol was used as a hydroxyl radical probe (k_{OH}• = 4.0 x 10^9) (*19*). Reactions were conducted in 20 mL borosilicate vials capped with PTFE-lined septa under minimal light at 20 ± 2˚C. Steady-state conditions were maintained by adding H_2O_2 or KO_2 every 5 minutes to restore the concentration to its initial level. A triplicate set of reactors was established for each time point in an experiment; as the reactions proceeded, the total reactor contents were extracted with hexane, and the extracts were analyzed by gas chromatography. The data were analyzed by averaging the results from triplicate reactors.

Reactivity of Hydroxyl Radical in MnO_2–H_2O_2 Systems. Reactions consisted of 10 mL of 2 mM 1-hexanol, 5 mg MnO_2, and 0.15 M H_2O_2; the pH, which was unadjusted, was 6.8. Control reactions were conducted in parallel using MnO_2 but with double deionized water in place of H_2O_2.

Reactivity of Superoxide in MnO_2–H_2O_2 Systems. Reactions consisted of 10 mL of 2 μM HCA, 5 mg MnO_2, and varied H_2O_2 concentrations (0.0075 M–0.15 M) at pH 6.8. Control

reactions were conducted in parallel using MnO_2 but with double deionized water in place of H_2O_2.

Reactivity of Superoxide in Iron (III)-EDTA–H_2O_2 Systems. Reactions consisted of 10 mL of 2 μM HCA, 5 mM iron (III)-EDTA, and varied H_2O_2 concentrations (0.025 M–1.2 M); the pH, which was unadjusted, was 6.5. Control reactions were conducted in parallel using iron (III)-EDTA, but with double deionized water in place of H_2O_2.

Reactivity of Superoxide in MnO_2–KO_2 Systems. Potassium superoxide was added to deionized water based on the methodology of Marklund (*10*). The reactions contained 15 mL of 2 μM HCA, 5 mg MnO_2, 33 mM purified NaOH, 1 mM DTPA (to bind and inactivate transition metals), and varied KO_2 concentrations (0.1, 0.2 and 0.4 M). Reactions were conducted at pH 14 to minimize the dismutation of superoxide. Control reactions without MnO_2 were conducted in parallel.

Reactivity of Superoxide in Glass Sphere–KO_2 Systems. Reactions contained 7.5 mL of 2 μM HCA, 7.5 g of soda-lime glass spheres of different diameters (41.5 μm, 82.5 μm and 165 μm), 33 mM purified NaOH, 1 mM DTPA, and 0.1 M KO_2 at pH 14. Control reactions were conducted in parallel without glass spheres. The specific surface area of the glass spheres was calculated using the soda-lime glass density of 2.44 g/cm^3 and assuming a perfect spherical shape (*20*).

Analysis. Hexane extracts were analyzed for HCA using a Hewlett-Packard 5890A gas chromatograph with a 0.53 mm (i.d.) × 60 m Equity 1 capillary column and electron capture detector (ECD). Chromatographic parameters included an injector temperature of 220˚C, detector temperature of 270˚C, initial oven temperature of 100˚C, program rate of 30˚C/min, and

final temperature of 240˚C. H_2O_2 and KO_2 concentrations were measured by iodometric titration (*1*).

Statistical Analysis. Statistical analyses were performed using the SAS software package version 9.1 (*21*). Linear regressions were performed to calculate first-order rate constants for HCA degradation. A contrast test was performed using a general linear model to compare regression coefficients (first-order rate constants for HCA degradation) across four different treatments in the KO_2–glass sphere systems.

Results and Discussion

Detection of Superoxide in MnO_2–H_2O_2 Systems. The presence of superoxide in MnO_2–H_2O_2 systems was confirmed by the addition of the spin trapping agent DMPO, followed by ESR spectroscopy analysis. Two DMPO radical adducts were observed in the ESR spectra (Figure 1): a superoxide adduct (DMPO–OOH) with hyperfine splitting constants of A_N = 14.36, A^{α}_H = 11.24, and A^{β}_H = 1.07–gauss, and a hydroxyl radical adduct (DMPO–OH) with hyperfine splitting constants of A_N =14.57 and A_H = 14.57. These results are consistent with ESR spectra and hyperfine splitting constants obtained for superoxide and hydroxyl radical in other studies (*22–24*), and confirm the presence of superoxide in MnO_2–H_2O_2 systems. The presence of the DMPO–OH adduct in the ESR spectra can be explained by two mechanisms: 1) generation of hydroxyl radical in the MnO_2–H_2O_2 systems, which then reacts with DMPO ($k = 2.1–5.7 \times 10^9$ $M^{-1}s^{-1}$), or 2) formation of DMPO–OH as a decomposition product of the superoxide adduct, DMPO–OOH (*24, 25–27*). Previous work has shown that hydroxyl radical is not generated in significant amounts in MnO_2–H_2O_2 systems containing the manganese oxide pyrolusite (*28*). To investigate whether hydroxyl radical is generated in the birnessite MnO_2–H_2O_2 systems used in

the present study, 1-hexanol was used as a hydroxyl radical probe (*28*). No degradation of 1-hexanol was observed (Figure 2); therefore, the DMPO–OH adduct is likely a decomposition product of the DMPO–OOH superoxide adduct.

These results confirm that superoxide is generated in the MnO_2–H_2O_2 systems used in this study. Similarly, Zhou et al. (*29*) observed a DMPO–OOH superoxide adduct in systems containing Fe_2O_3, NaOH, H_2O_2, and DMPO; they suggested that the primary mechanism responsible for superoxide formation was heterogeneous surface decomposition of H_2O_2 initiated by iron oxides.

Reactivity of Superoxide in MnO_2–H_2O_2 and Iron (III)-EDTA–H_2O_2 Systems. Hexachloroethane was used as a superoxide probe to investigate the reactivity of superoxide in MnO_2 systems with varying concentrations of H_2O_2. The degradation of HCA in MnO_2 systems containing 7.5–150 mM H_2O_2 is shown in Figure 3. HCA degradation increased as a function of H_2O_2 concentration, and followed first-order kinetics at all of the concentrations investigated. The first-order rate constants for HCA degradation, derived from the slope of $\ln[HCA]/[HCA]_0$ vs. time, were proportional to H_2O_2 concentrations between 0–50 mM (Figure 4). These data are in agreement with the results of Ono et al. (*15*), who observed increasing superoxide generation with increasing H_2O_2 concentrations in the presence of several metal oxides. At H_2O_2 concentrations > 50 mM, the rate of HCA degradation did not increase further; these results likely demonstrate saturation kinetics with respect to superoxide generation at the mineral surface (*30*).

The Eley-Rideal kinetic model was used to examine the generation of superoxide and its reactivity with HCA in the H_2O_2-birnessite system. Reactions 7-10 serve as the basis for the model.

$$H_2O_2 \overset{MnO_2}{\underset{k-}{\overset{k_1}{\rightleftharpoons}}} H_2O_{2sorbed} \qquad K_1 \tag{7}$$

$$H_2O_{2sorbed} \overset{k_2}{\underset{k_{-2}}{\rightleftharpoons}} O_2\cdot^-_{sorbed} \qquad K_2 \tag{8}$$

$$O_2\cdot^-_{sorbed} \xrightarrow{HCA} \text{Products} \qquad k_3 \tag{9}$$

$$O_2\cdot^- \overset{MnO_2}{\underset{k'_{-1}}{\overset{k'_1}{\rightleftharpoons}}} O_2\cdot^-_{sorbed} \qquad K'_1 \tag{10}$$

where K_1 = adsorption coefficient for H_2O_2,
k_1 = sorption rate for H_2O_2,
k_{-1} = desorption rate for H_2O_2,
k_2 = decomposition of hydrogen peroxide with the formation of superoxide on the surface,
k_{-2} = dismutation rate for superoxide on the surface,
K_2 = equilibrium constant for the reaction [8],
k_3 = reaction rate for the reaction between superoxide and HCA,
K'_1 = the adsorption coefficient for superoxide,
k'_1 = sorption rate for O^-_2,
k'_{-1} = desorption rate for O^-_2,

The assumptions of the model are as follows: reactions 7 through 10 take place at the catalyst surface; the initial rate of superoxide formation is proportional to the concentration of H_2O_2 (*15*); the concentration of superoxide is at steady-state; $K_1 = K_{H_2O_2} \approx 1\ M^{-1}$; $k_{-2} < k_2$; and $k_{-2} < k_3$. The Eley-Rideal mechanism for the reaction between sorbed superoxide and aqueous HCA, provides the following equation:

$$\frac{1}{k_{obs}} = \frac{1}{k_3 \cdot \frac{k_2 \cdot K_1}{(k_{-2} + k_3)} \cdot [H_2O_2]} + \frac{1}{k_3} \tag{11}$$

The derivation of equation 11 is shown in the Supplemental Information (Appendix 1). The kinetic constants K_1, k_2, k_{-2}, and k_3 have not been established to date, so equation (11) cannot be

used as a predictive model. However, equation (11) was used to confirm the data of Figure 4, and to approximate k_3 and k_2 for the data. A Lineweaver-Burk type plot of $\frac{1}{k_{obs}}$ (min) *vs.* $\frac{1}{[H_2O_2]}$ (mM^{-1}) yielded a y-intercept ($1/k_3$) of 11.4 min; therefore, $k_3 = 0.0015\ s^{-1}$. The slope was 294 min·mM ($R^2 = 0.99$), yielding an approximate k_2 of $0.057\ M^{-1}\ s^{-1}$.

The results of Figures 3 and 4 suggest that the increasing HCA degradation seen with increasing H_2O_2 concentrations was due to greater generation of superoxide on the mineral surface. However, superoxide is not reactive in pure water (*11*); therefore, one or more components of the MnO_2–H_2O_2 systems must increase the lifetime and reactivity of superoxide.

The results of Figures 3 and 4 demonstrate that superoxide was reactive at low H_2O_2 concentrations (e.g., 7.5 mM) in a heterogeneous system; however, much higher concentrations of H_2O_2 (e.g., > 100 mM) are required for superoxide reactivity in homogeneous systems such as aqueous KO_2 systems or soluble iron-catalyzed CHP reactions (*1*). Reactions were repeated in a homogeneous CHP system in order to directly compare the effect of H_2O_2 concentration on superoxide reactivity in heretogeneous (MnO_2) and homogeneous systems. Homogeneous CHP reactions, with H_2O_2 decomposition catalyzed by soluble iron rather than MnO_2, were conducted with varying concentrations of H_2O_2 (Figure 5). HCA degradation in the presence of 25 mM H_2O_2 was not significantly different from control systems ($p < 0.01$) while at H_2O_2 concentrations ≥ 100 mM, HCA degradation increased as a function of the H_2O_2 concentration. Because much higher concentrations of H_2O_2 were required to degrade HCA in the homogeneous iron(III)-EDTA catalyzed systems compared to the heterogeneous MnO_2-catalyzed systems, it is likely that H_2O_2 in the MnO_2–H_2O_2 systems was not solely responsible for the reactivity of superoxide with HCA. It is possible that the birnessite surface, in addition to catalyzing superoxide generation, also acted to increase superoxide reactivity.

Reactivity of Superoxide in MnO_2–KO_2 Systems. To investigate the effect of the MnO_2 surface on superoxide reactivity independent of the effect of the surface on superoxide generation, superoxide was directly added to the system as KO_2. Superoxide reactivity in aqueous 0.1 M KO_2 systems with and without MnO_2, as measured by loss of the probe HCA, is shown in Figure 6. The linear relationship between $\ln[HCA]/[HCA]_0$ and time demonstrates first-order degradation kinetics with respect to HCA in both KO_2 alone and MnO_2–KO_2 systems; however, the HCA degradation rate was approximately two times greater in the presence of MnO_2. The experiments were repeated using 0.2 and 0.4 M KO_2, and a linear correlation was evident between the first-order rate constants for HCA degradation and KO_2 concentrations in both KO_2 alone and MnO_2–KO_2 systems (Figure 7). As in Figure 6, the rate constants for HCA degradation in the MnO_2–KO_2 reactions were significantly higher than in systems with only KO_2 ($p < 0.01$). Such findings are consistent with previous studies that have shown superoxide to be stabilized in the presence of other metal oxides (*12, 14, 31*). These results provide strong evidence that superoxide reactivity is increased in the presence of MnO_2, and raise the possibility that other solids may also increase superoxide reactivity in water.

Reactivity of Superoxide in Glass Sphere–KO_2 Systems. To further investigate the effect of solid surfaces on superoxide reactivity, glass beads of varying surface area were added to aqueous 0.1 M KO_2 systems. The relative reactivity of superoxide in glass sphere–KO_2 systems, quantified by the loss of HCA, is shown in Figure 8. Degradation of HCA increased significantly in glass sphere–KO_2 systems containing 0.015 and 0.030 m^2/g glass surface area relative to the system with only KO_2 ($p < 0.01$), and was greater with 0.059 m^2/g glass surface area ($p < 0.01$). Superoxide reactivity, as measured by first-order rate constants for HCA degradation, was directly proportional to the surface area of the glass spheres (Figure 9).

Konecny et al. (*32*) demonstrated that superoxide sorbs to silica quartz surfaces, and such sorption may have a role in the increased reactivity of superoxide in the presence of glass spheres.Using the birnessite surface area of 50.6 m^2/g, the rate constant for the degradation of HCA in 0.1 M KO_2-MnO_2 was included in Figure 9. The datum for KO_2-MnO_2 HCA degradation falls directly on the line describing increased superoxide reactivity as a function of glass bead surface area. This relationship suggests that the surface area of the solid, rather than the nature of the surface, is responsible for increased superoxide reactivity in solid–superoxide systems.

The results of this research demonstrate that the presence of solids in aqueous systems increased the reactivity of superoxide, whether the superoxide was generated through catalytic decomposition of H_2O_2 by MnO_2, or through the addition of KO_2 to MnO_2 or inert glass spheres. A linear relationship was demonstrated between the degradation rate of the superoxide probe HCA and the surface area of the glass spheres, confirming that solid surfaces enhance superoxide reactivity. Possible mechanisms of enhanced superoxide reactivity include catalytic effects at the solid surface, increased lifetime of superoxide in the solid surface microenvironment, changes in the solvation shell morphology of sorbed superoxide, and enhanced juxtaposition of organic compounds (e.g., HCA) with superoxide at solid surfaces, resulting in increased reactivity. These results have important implications for ISCO processes; superoxide generated in the presence of soils or subsurface solids may have increased reactivity with highly oxidized contaminants such as perchloroethylene and carbon tetrachloride, increasing the effectiveness of CHP ISCO. Furthermore, aqueous superoxide systems containing various surfaces could potentially be used for the treatment of industrial waste streams or waters containing micropollutants or xenobiotics.

Acknowledgements. Funding for this research was provided by Strategic Environmental Research and Development Program Project No. ER-1288.

Literature Cited

(1) Smith, B. A.; Teel, A. L.; Watts, R. J. Identification of the reactive oxygen species responsible for carbon tetrachloride degradation in modified Fenton's systems. *Environ. Sci. Technol.* **2004,** *38*, 5465-5469.

(2) Watts, R. J.; Bottenberg, B. C.; Jensen, M. E.; Hess, T. H.; Teel, A. L. Mechanism of the enhanced treatment of chloroaliphatic compounds by Fenton-like reactions. *Environ. Sci. Technol.* **1999,** *33*, 3432-3437.

(3) Watts, R. J.; Howsawkeng, J.; Teel, A. L. Destruction of a carbon tetrachloride dense nonaqueous phase liquid by modified Fenton's reagent. *J. Environ. Eng.* **2005,** *131*, 1114-1119.

(4) Watts, R. J.; Teel, A. L. Treatment of contaminated soils and groundwater using ISCO. *Pract. Period. Haz. Waste Manag.* **2006**, 2-9.

(5) Siegrist, R. L.; Urynowicz, M. A.; West, O. R.; Crimi, M. L.; Lowe, K. S. *Principles and practices for in situ chemical oxidation with permanganate*. Battelle Press: Columbus, Ohio, 2001.

(6) Teel, A. L.; Watts, R. J. Degradation of carbon tetrachloride by Fenton's reagent. *J. Hazard. Mater.* **2002**, *B94*, 179-189.

(7) Afanas'ev, I. B. *Superoxide ion: chemistry and biological implications Vol. 1*; CRC Press: Boca Raton, FL, 1989.

(8) Sawyer, D. T.; Martell, A. E. *Industrial environmental chemistry. Waste minimization in industrial processes and remediation of hazardous waste*. Plenum Press: New York, 1992.

(9) Bielski, B. H. J.; Allen, O. Mechanisms of the disproportionation of superoxide radicals. *J. Phys. Chem.* **1977,** *81*, 1048-1050.

(10) Marklund, S. Spectrometric study of spontaneous disproportionation of superoxide anion radical and sensitive direct assay for superoxide dismutase. *J. Biol. Chem.***1976,** *251*, 7504-7507.

(11) Sawyer, D. T.; Valentine, J. S., How super is the superoxide? *Acc. Chem. Res.* **1981,** *14*, 393-400.

(12) Anpo, M.; Che, M.; Fubini, B.; Garrone, E.; Giamello, E.; Paganini, M. C. Generation of superoxide ions at oxide surfaces. *Top. Catal.* **1999,** *8*, 189-198.

(13) Kitajima, N.; Fukuzumi, S.-I.; Ono, Y. Formation of superoxide ion during the decomposition of hydrogen peroxide on supported metal oxides. *J. Phys. Chem.* **1978,** *82*, 1505-1508.

(14) Giamello, E.; Calosso, L.; Fubini, B.; Geobaldo, F. Evidence of stable hydroxyl radicals and other oxygen radical species generated by interaction of hydrogen peroxide with magnesium oxide. *J. Phys. Chem.* **1993,** *97*, 5735-5740.

(15) Ono, Y.; Matsumura, T.; Kitajima, N.; Fukuzumi, S.-I. Formation of superoxide ion during the decomposition of hydrogen peroxide on supported metals. *J. Phys. Chem.* **1977,** *81*, 1307-1311.

(16) Das, K. C.; Misra, H. P. Hydroxyl radical scavenging and singlet oxygen quenching properties of polyamines. *Mol. Cell. Biochem.* **2004,** *262*, 127-133.

(17) McKenzie, R. M. Manganese oxides and hydroxides. In *Minerals in Soil Environments*, 2nd ed.; Dixon, J.B., Weed, S. B., Ed.; SSSA Book Series, SSSA: Madison, 1989.

(18) Brunauer, S..; Emmett, P. H.; Teller, E. Adsorption of gases in multi-molecular layers. *J. Am. Chem. Soc.* **1938,** *60*, 309-319.

(19) Buxton, G. V.; Greenstock, C. L.; Helman, W. P.; Ross, A. B. Critical review of rate constants for reactions of hydrated electrons, hydrogen atoms and hydroxyl radicals ($\bullet OH/\bullet O^-$) in aqueous solution. *J. Phys. Chem. Ref. Data* **1988**, *17*, 513-780.

(20) Hillel, D. *Environmental Soil Physics*. Academic Press: San Diego, 1998.

(21) *The SAS system for Windows*, Release 9.1.; SAS Institute: Cary, NC, 2003.

(22) Finkelstein, E.; Rosen, G. M.; Rauckman, E. J. Spin trapping. Kinetics of the reaction of the superoxide and hydroxyl radicals with nitrones. *J. Am. Chem. Soc.* **1980,** *102*, 4994-4999.

(23) Yim, M. B.; Berlett, B. S.; Chock, P. B.; Stadtman, E. R. Manganese (II)-bicarbonate-mediated catalytic activity for hydrogen peroxide dismutation and amino acid oxidation: detection of free radical intermediates. *Proc. Natl. Acad. Sci. U. S. A.* **1990,** *87*, 394-398.

(24) Zhao, H.; Joseph, J.; Zhang, H.; Karoui, H.; Kalyanaraman, B. Synthesis and biochemical applications of a solid cyclic nitrone spin trap: a relatively superior trap for detecting superoxide anions and glutathiyl radicals. *Free Radical Biol. Med.* **2001,** *31*, 599-606.

(25) Finkelstein, E.; Rosen, G. M.; Rauckman, E. J. Production of hydroxyl radical by decomposition of superoxide spin-trapped adducts. *Mol. Pharmacol.* **1982,** *21*, 262-265.

(26) Shi, H.; Timmins, G.; Monske, M.; Burdick, A.; Kalyanaraman, B.; Liu, Y.; Clement, J.-L.; Burchiel, S.; Liu, K. J. Evaluation of spin trapping agents and trapping conditions for detection of cell-generated reactive oxygen species. *Arch. Biochem. Biophys.* **2005,** *437*, 59-68.

(27) Turner, M. J.; Rosen, G. M. Spin trapping of superoxide and hydroxyl radicals with substituted pyrriline 1-oxides. *J. Med. Chem.* **1986,** *29*, 2439-2444.

(28) Watts, R. J.; Sarasa, J.; Loge, F. J.; Teel, A. L. Oxidative and reductive pathways in manganese-catalyzed Fenton's reactions. J. Environ. Eng. **2005**, *131*, 158-164.

(29) Zhou, N.; Qiu, T.; Yang-Ping, L.; Yang, L. Superoxide anion radical generation in the NaOH/H2O2/Fe(III) system: a spin trapping ESR study. *Magn. Reson. Chem.* **2006,** *44*, 38-44.

(30) Zhou, H.; Shen, Y.F.; Wang, J.Y.; Chen, X.; O'Young, C.-L.; Suib, S.L. Studies of decomposition of H_2O_2 over manganese oxide octahedral molecular sieve materials. *J. Catal.* **1998**, *176*, 321-328.

(31) Zhang, X.; Klabunde, K. J. Superoxide on the surface of heat-treated ceria. Intermediates in the reversible oxygen to oxide transformation. *Inorg. Chem.* **1992,** *31*, 1706-1709.

(32) Konecny, R.; Leonard, S.; Shi, X.; Robinson, V.; Castranova, V. Reactivity of free radicals on hydroxylated quartz surface and its implications for pathogenicity of silicas: experimental and quantum mechanical study. *J. Environ. Pathol. Toxicol. Oncol.* **2001,** *20*, 119-132.

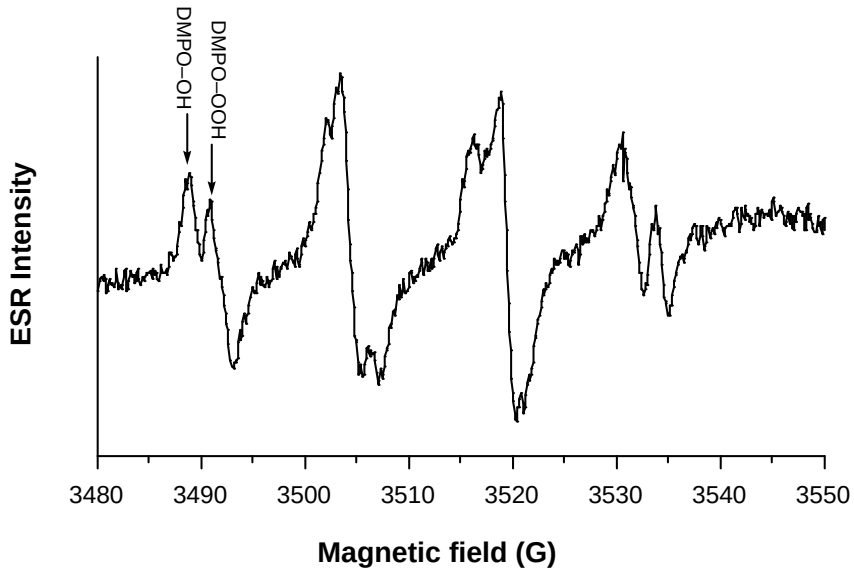

Figure 1. Electron spin resonance spectra of DMPO-OOH (A_N=14.36, A^{β}_H=11.24, A^{α}_H=1.07-gauss) and DMPO-OH (A_N=14.57, A_H=14.57) adducts in MnO_2–H_2O_2 systems (reactors: 1 mg MnO_2, 0.2 M H_2O_2 and 0.18 M DMPO; total volume of 2.5 mL at pH 6.8; T = 20 ± 1˚C).

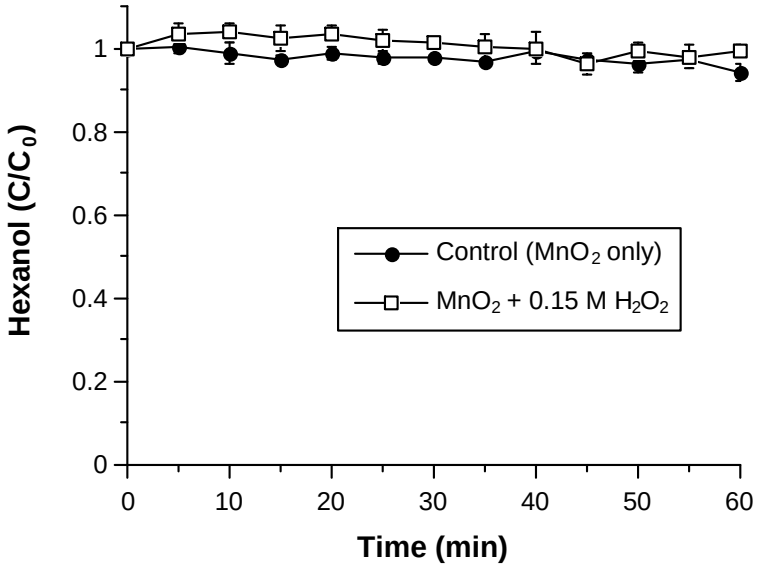

Figure 2. Degradation of hexanol in MnO_2–H_2O_2 systems (experimental reactors: 2 mM 1-hexanol, 5 mg MnO_2, and 0.15 M H_2O_2; 10 mL total volume at pH 6.8; control reactors: H_2O_2 substituted by deionized water; T = 20 ± 1˚C). Error bars represent the standard error of the mean for three replicates.

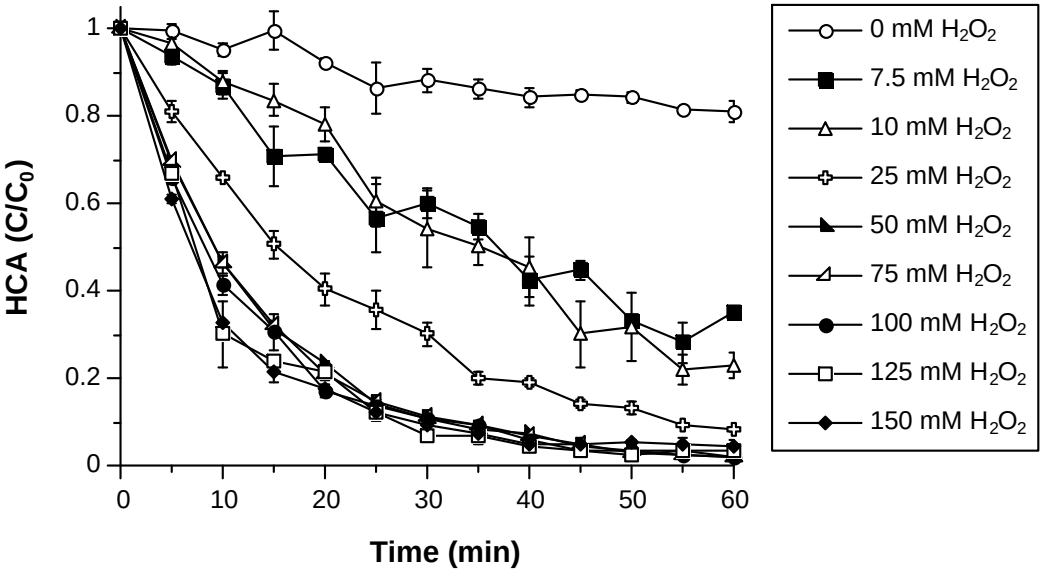

Figure 3. Degradation of HCA in MnO_2–H_2O_2 systems with varying H_2O_2 concentrations (experimental reactors: 2 μM HCA, 5 mg MnO_2, and 0–150 mM H_2O_2; 10 mL total volume at pH 6.8; control reactors: H_2O_2 substituted by deionized water; T = 20 ± 1˚C). Error bars represent the standard error of the mean for three replicates.

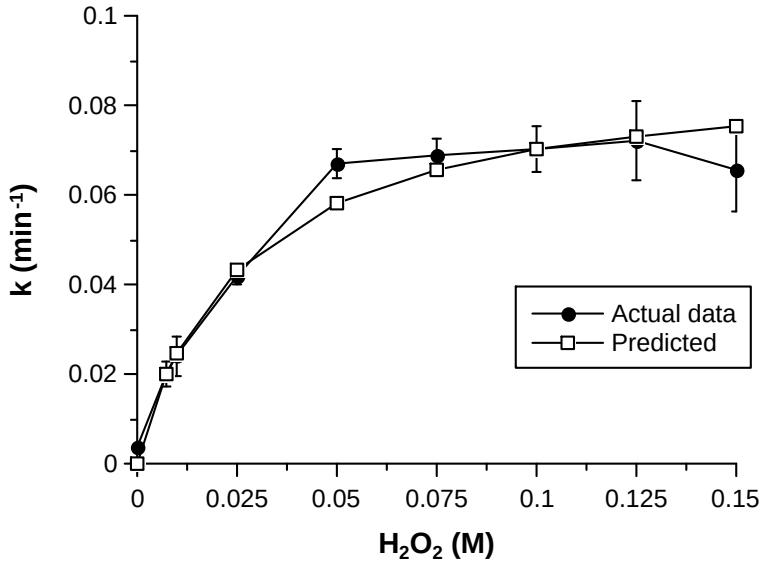

Figure 4. Correlation of first order rate constants for HCA degradation with H_2O_2 concentrations in MnO_2–H_2O_2 systems. Error bars on the data points represent 95% confidence intervals for the linear regressions. The predicted data were developed from Eq. 11.

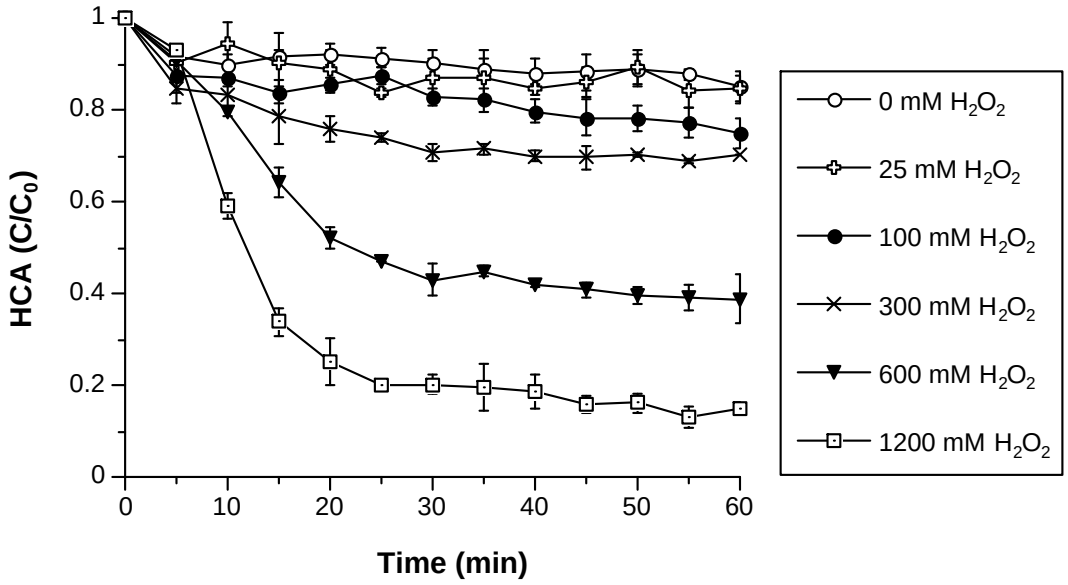

Figure 5. Degradation of HCA in iron (III)-EDTA–H_2O_2 systems with varying H_2O_2 concentrations (experimental reactors: 2 μM HCA, 5 mM iron (III)-EDTA, and 0–1200 mM H_2O_2; 10 mL total volume at pH 6.8–6.9; control reactors: H_2O_2 substituted by deionized water; T = 20 ± 1˚C). Error bars represent the standard error of the mean for three replicates.

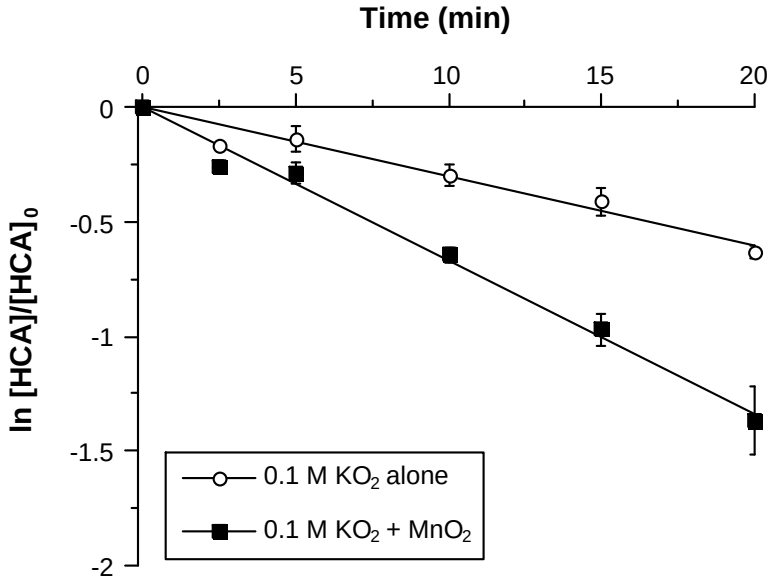

Figure 6. Degradation of HCA in MnO_2–KO_2 systems with and without manganese oxide (experimental reactors: 2µM HCA, 0.1 M KO_2, 33 mM NaOH, 1 mM DTPA, and 5 mg MnO_2 [0.0167 m_2/mL surface area]; 15 mL total volume at pH 14; control reactors: no MnO_2; T = 4 ± 1˚C). Error bars represent the standard error of the mean for three replicates.

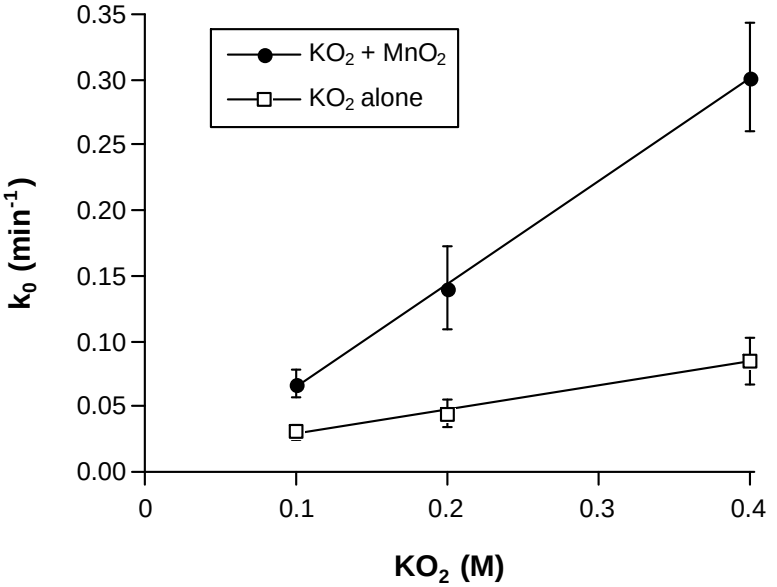

Figure 7. Relationship between KO_2 concentrations and first-order rate constants for HCA degradation in KO_2-MnO_2 and aqueous KO_2 systems. Error bars represent 95% confidence intervals for the linear regressions.

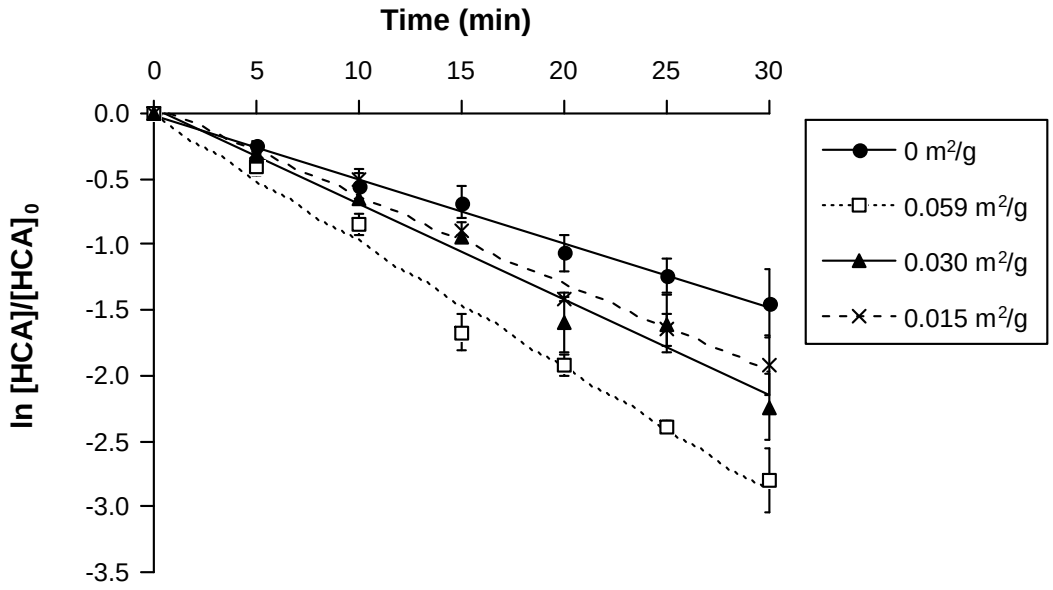

Figure 8. The surface area of glass spheres effect on HCA degradation in KO_2 reactions: 0.1 M KO_2, 1 g/mL glass spheres, 2μ M HCA. Error bars represent the standard error of the mean for three replicates.

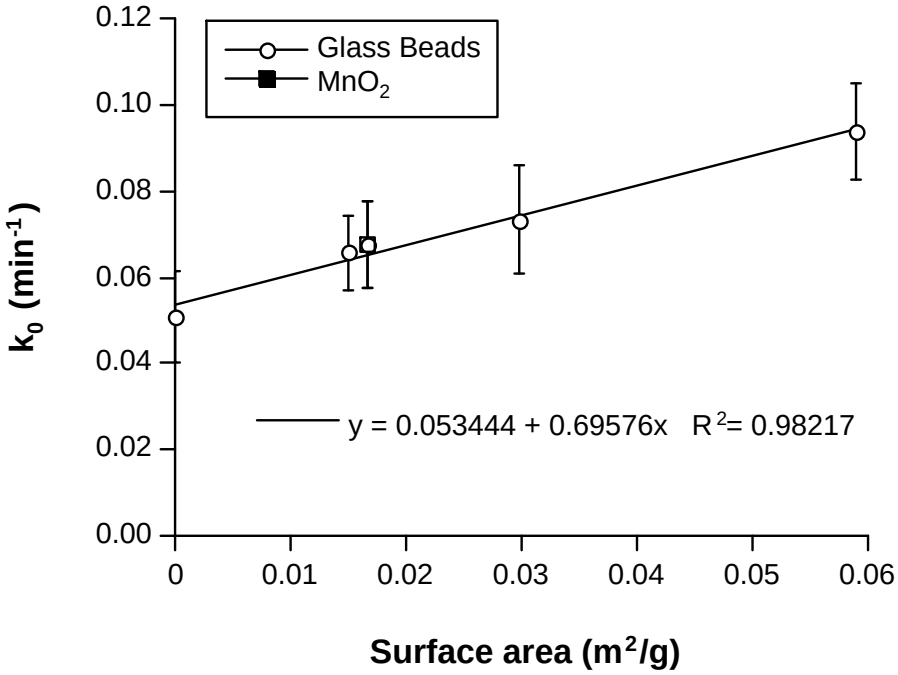

Figure 9. Relationship between the surface area of glass beads and manganese oxide and first-order rate constants for HCA degradation in a 0.1 M KO_2 system (R^2 = 0.99). Error bars represent 95% confidence intervals for the linear regressions.

CHAPTER 4: MECHANISM OF BASE-ACTIVATION OF PERSULFATE

Introduction

In situ chemical oxidation (ISCO) has become a widely used technology for the remediation of contaminated soils and groundwater. The most common oxidation processes used for ISCO are catalyzed H_2O_2 propagations (CHP), permanganate, ozone, and activated persulfate *(1)*. Persulfate is an increasingly popular ISCO reagent because it is significantly more stable than hydrogen peroxide, providing the potential for oxidant transport from the point of injection to contaminants in lower permeability regions of the subsurface. Activated persulfate is a strong oxidant capable of degrading most contaminants of concern *(2-6)*. For example, activated persulfate effectively destroys organic contaminants such as trichloroethylene, trichloroethane, methyl *tert*-butyl ether, polychlorinated biphenyls, and BTEX *(4, 5, 7, 8)*. Persulfate ion ($S_2O_8^{2-}$) undergoes decomposition/activation to produce the reactive oxygen species in the presence of metals, some organic compounds (aliphatic and aromatic compounds), heat, and light *(2, 9)*.

Base activation of persulfate is one of the most common ISCO practices and has been used at ~60% of sites where persulfate ISCO was employed *(10)*. Base-activated persulfate technology has been successfully applied for the destruction of recalcitrant chlorinated methanes and ethanes in the groundwater and soil systems when base was used in excess *(11, 12)*. Several mechanisms of base activation of persulfate have been proposed *(13-15)*, but none of them have been confirmed. The objective of this study was to elucidate the mechanism of base activation of persulfate in strongly alkaline conditions.

Experimental Section

Materials. Sodium persulfate (98%), sodium perchlorate (99%), hexachloroethane (HCA) (99%), and diethylenetriaminepentaacetic acid (DTPA) (97%) were purchased from Sigma-

Aldrich (St. Louis, MO). 5,5-Dimethyl-1-pyrroline-N-oxide (DMPO) (≥ 99%) was obtained from Axxora LLC (San Diego, CA). The impurities in DMPO were removed with activated charcoal followed by filtration until no extraneous electron spin resonance spectroscopy (ESR) signals were observed *(16)*. Magnesium chloride (99.6%), hydrogen peroxide (50%), sodium hydroxide (98%), sulfuric acid (96.1%), acetic acid (> 99%), sodium bicarbonate (> 99%), ammonium sulfate (> 99%). and starch were obtained from J.T. Baker (Phillipsburg, NJ). Stock solutions of peroxomonosulfate (SO_5^{2-}) were prepared from oxone ($2KHSO_5 \cdot KHSO_4 \cdot K_2SO_4$), which was obtained from Alfa Aesar (Ward Hill, MA). Potassium iodide (99%) was purchased from Alfa Aesar (Ward Hill, MA), and titanium sulfate was obtained from GFS Chemicals, Inc. (Columbus, OH). Mixed hexanes (60%) and sodium thiosulfate (> 99%) were purchased from Fisher Scientific (Fair Lawn, NJ). Double-deionized water was purified to > 18 MΩ•cm using a Barnstead E-pure system. Sodium hydroxide solutions were purified to remove transition metals by the addition of magnesium chloride followed by stirring for 8 hours and then filtering the solution through 0.45 μm hydrophilic polypropylene membrane filters *(17, 18)*.

Persulfate Decomposition Studies. Persulfate concentrations were measured by iodometric titration with 0.01 N sodium thiosulfate *(19)* in solutions containing varied concentrations of NaOH and $NaClO_4$ to examine sodium hydroxide and ionic strength effects on sodium persulfate decomposition in strongly alkaline conditions.

Measurement of Oxygen Evolution. A U-tube manometer filled with water was used to measure the differential pressure in reactions containing 1) 0.25 M persulfate, 3M NaOH, 2) 0.5 M persulfate, 3 M NaOH, and 3) 0.5 M persulfate, 1.5 M NaOH. A reactor was attached to one end of the U-tube manometer, and the other end of the U-tube was open to the atmosphere. The

ideal gas law was applied to calculate the amount of oxygen evolved over time during the reaction. Persulfate concentrations were measured in parallel by iodometric titration.

Detection of Peroxomonosulfate. Peroxomonosulfate ion concentrations were measured in the reactions using a Metrohm model 690 ion chromatograph equipped with a Super-Sep anion-exchange column. The mobile phase consisted of a degassed solution of 2.0 mmol/L phthalic acid containing 5% (v/v) acetonitrile (pH 3); the flow rate of the mobile phase was 1.5 ml/min *(20)*.

Reactivity of HO_2^- in Persulfate–NaOH Systems. Reactions consisted of 20 mL of 0.5 M persulfate, 0.5 M–1.5 M NaOH, and 0.5–1 M H_2O_2, which dissociates to HO_2^- in highly alkaline systems. Hydrogen peroxide/hydroperoxide decomposition was monitored in the persulfate –NaOH reactions under a range of concentrations of NaOH and H_2O_2.

Sodium persulfate and hydrogen peroxide concentrations were also monitored simultaneously in the reaction of 0.5 M persulfate, 1.5 M NaOH, and 0.5 H_2O_2 to examine the stoichiometry of reaction of HO_2^- and persulfate. Hydrogen peroxide concentrations were quantified after complexation with titanium sulfate followed by a spectrophotometric analyses at 407 nm using Spectronic 20 Genesys spectrophotometer *(21, 22)*. Iodometric quantification of persulfate also measures hydrogen peroxide; the concentration of hydrogen peroxide as determined by Ti(IV) sulfate complexation was subtracted from the total peroxygen concentration to obtain the concentration of persulfate.

Generation of Superoxide in Persulfate-NaOH-H_2O_2 Systems. HCA was used as a probe for superoxide reactivity *(23)*. Reactions consisted of 20 mL of 2 μM HCA, 0.5 M persulfate, 1 M NaOH, and H_2O_2 concentrations ranging from 0.1 M–0.5 M. Control reactions were conducted in parallel with double deionized water in place of H_2O_2. Reactions were

conducted in borosilicate vials capped with PTFE-lined septa under minimal light at 20 ± 2˚C. A triplicate set of reactors was established for each time point in an experiment; as the reactions preceded, the total reactor contents were extracted with hexane, and the extracts were analyzed by gas chromatography.

Detection of Radicals Using ESR Spectroscopy. Radicals were detected with ESR spectroscopy using DMPO as a spin trap agent. The reaction mixture for ESR spin trapping consisted of 3 mL of 0.05 M persulfate, 0.1 M NaOH, 5 mM DTPA, and 0.15 M DMPO. DTPA (5mM) was added to eliminate the effects of metal impurities on radical generation. The reactants were injected into an aqueous sample cell (Bruker, AquaX high sensitivity) 1 min after the reaction was initiated. All spectra were obtained using a Bruker 6/1 spectrometer with a resonance frequency of 9.86 GHz, microwave power of 2.0 mW, modulation frequency of 100 kHz, modulation amplitude of 1.0 G, sweep width of 100 G, time constant of 164 ms, sweep time of 168 s, and receiver gain of 2.0×10^5.

Probe Compound Analysis. Hexane extracts were analyzed for HCA using a Hewlett-Packard 5890A gas chromatograph with a 0.53 mm (i.d.) × 60 m Equity 1 capillary column and electron capture detector (ECD). Chromatographic parameters included an injector temperature of 220˚C, detector temperature of 270˚C, initial oven temperature of 100˚C, program rate of 30˚C/min, and final temperature of 240˚C.

Statistical Analysis. Statistical analyses were performed using the SAS software package version 9.1 *(24)*. Linear regressions were performed to calculate first-order rate constants for persulfate decomposition. A contrast test was performed using a general linear model to compare regression coefficients (first-order rate constants for persulfate decomposition) across different treatments.

Results and Discussion

Proposed Mechanism. The proposed mechanism is based on the nucleophilic attack of hydroxide on persulfate with subsequent formation of hydroperoxide and sulfate ions. Hydroperoxide then reduces another persulfate molecule, generating sulfate radical, sulfate ion, and superoxide. A significant degree of scavenging likely occurs, resulting in sulfate and oxygen as end products.

Base activation:

$^{-}{}_3OS\text{-}O\text{-}O\text{-}SO_3^{-} + 2OH^{-} \longrightarrow HO_2^{-} + SO_4^{2-} + HSO_4^{-}$ [1]

$^{-}{}_3OS\text{-}O\text{-}O\cdots SO_3^{-} + OH^{-} \xrightarrow{k_1} {}^{-}{}_3OS\text{-}O\text{-}O^{-} + HSO_4^{-}$ **Transition state** [2]

$^{-}{}_3OS\text{-}O\text{-}O^{-} + OH^{-} \longrightarrow H\text{-}O\text{-}O^{-} + SO_4^{2-}$ [3]

$H\text{-}O\text{-}O^{-} + {}^{-}{}_3OS\text{-}O\text{-}O\text{-}SO_3^{-} \xrightarrow{k_2} SO_4^{\bullet -} + HSO_4^{-} + O_2^{\bullet -}$ [4]

Scavenging of radicals:

$2O_2^{\bullet -} \xrightarrow{H_2O} O_2 + OH^{-} + HO_2^{-}$ $<1\ M^{-1}s^{-1}$ (pH>13) [5]

$SO_4^{\bullet -} + OH^{-} \longrightarrow SO_4^{2-} + OH^{\bullet}$ $7.3 \times 10^7\ M^{-1}s^{-1}$ [6]

$SO_4^{\bullet -} + O_2^{\bullet -} \longrightarrow SO_4^{2-} + O_2$ [7]

$OH^{\bullet} + OH^{-} \longrightarrow O^{\bullet -} + H_2O$ $1.3 \times 10^{10}\ M^{-1}s^{-1}$ [8]

$O^{\bullet -} + O_2^{\bullet -} + H_2O \longrightarrow O_2 + 2\ HO^{-}$ $6.0 \times 10^8\ M^{-1}s^{-1}$ [9]

$OH^{\bullet} + SO_4^{\bullet -} \longrightarrow HSO_4^{-} + \frac{1}{2}\ O_2$ [10]

$OH^{\bullet} + O_2^{\bullet -} \longrightarrow O_2 + OH^{-}$ $(8\text{-}10) \times 10^9\ M^{-1}s^{-1}$ [11]

$2OH^{\bullet} \longrightarrow 1/2\ O_2 + H_2O$ [12]

Sodium Persulfate Decomposition Kinetics. Sodium persulfate decomposition was examined at four different NaOH concentrations. The reactions contained 0.5 M persulfate and 1 M, 1.5 M, 2 M, or 3 M NaOH for molar ratios of NaOH:persulfate of 2:1, 3:1, 4:1, and 6:1.

Persulfate decomposition followed first-order kinetics under basic conditions (Figure 1), and the rate of persulfate decomposition increased as a function of the sodium hydroxide concentration. These results confirm that hydroxide has a dominant role in the decomposition of persulfate. A plot of the first order rate constants for persulfate decomposition as a function of the natural log of sodium hydroxide concentration is shown in Figure 2. The results demonstrate a linear relationship, and suggest that the order of the reaction with respect to hydroxide is close to 2. Therefore, persulfate likely consumes two hydroxides molecules during its decomposition. The initial step of persulfate decomposition is likely a second order reaction, reaction [2], between persulfate and hydroxide followed by reaction [3] in which a second hydroxide is consumed resulting in the following rate expression:

$$\frac{-d\left[Na_2S_2O_8\right]}{dt} = k_1\left[OH^-\right]^2\left[Na_2S_2O_8\right]$$ **rate-limiting step**

Effect of Ionic Strength. The rate of persulfate decomposition at varying ionic strengths was examined in a 3 M sodium hydroxide solution at different sodium perchlorate concentrations. The first-order rate for persulfate decomposition increased as ionic strength increased. These results are in accordance with Debye-Huckel-Bronsted theory of ionic reaction and demonstrate a positive salt effect, which indicates that the rate-determining step is the reaction between two negatively charged ions (e.g., persulfate and hydroxide) *(13)*.

Evolution of Oxygen. Oxygen evolution during base activated persulfate reactions with two different persulfate and NaOH concentrations is shown in Figure 4. The rate of oxygen evolution increased as a function of sodium hydroxide concentration, and also increased with persulfate concentrations. These results are in agreement with the data shown in Figure 1 in that increased base concentrations promoted an increased rate of persulfate decomposition and concomitant oxygen evolution.

Summing reactions [2] and [4] yields the following net reaction:

$2S_2O_8^{2-} + 2\ OH^- \longrightarrow 2HSO_4^- + SO_4^{2-} + SO_4^{\bullet-} + O_2^{\bullet-}$

In highly alkaline conditions, sulfate radicals proceed via reaction [6] to form hydroxyl radicals. Superoxide radicals are likely scavenged through reactions [7], [9], and [11], yielding oxygen. Therefore, the evolved oxygen would be expected to follow the stoichiometry:

$2\ S_2O_8^{2-} \longrightarrow O_2$

The ratio of persulfate consumed to oxygen evolved in the reaction containing 0.5 M persulfate and 3 M NaOH is shown in Figure 5. As expected, the ratio reached 0.5, for two moles of persulfate consumed per mole of oxygen evolved. The same ratio was found for the other persulfate and NaOH concentrations used in Figure 4 (data not shown). The predicted and measured results are in high agreement, providing more evidence for the proposed mechanism.

Reactivity of Hydroperoxide Anion. Equation [3] of the proposed mechanism suggests that the peroxomonosulfate ion is formed during the base-catalyzed hydrolysis of persulfate. Peroxomonosulfate ion was not detected by ion chromatography in solutions containing persulfate and sodium hydroxide at varying concentrations (data not shown). However, several studies have demonstrated that peroxomonosulfate undergoes rapid decomposition at basic pH (*25-27*). Therefore, peroxomonosulfate ion would not be expected to be stable in base activated persulfate systems at high pH. Persulfate likely forms an activated complex with hydroxide that weakens the S—O bond [2]. As a result, the S—O bond undergoes fission, and hydroperoxide and sulfate ions are formed [3].

In the proposed mechanism, HO_2^- is generated through reaction [3]; however, HO_2^- was non-detectable by Ti(IV) sulfate complexation *(21)*. Other methods typically used to detect H_2O_2/HO_2^- such as iodometric titration or catalase could not be used in these systems because of

interference from persulfate. Persulfate decomposes relatively slowly, with an estimated rate of ~3.3×10^{-3} mM/min in a solution of 0.5 M persulfate and 3 M NaOH. Therefore, HO_2^- would be generated through reaction [3] at a rate of less than 3.3×10^{-3} mM/min; if HO_2^- is subsequently consumed at a rate more rapid than its production, it would be undetectable in the system.

To evaluate the fate of hydroperoxide that might be generated through the base-catalyzed hydrolysis of persulfate, external hydroperoxide addition was investigated from two standpoints: 1) the fate of hydroperoxide after its addition to basic persulfate systems, and 2) the effect of adding extra hydroperoxide on free radical based reactions. Hydroperoxide concentrations decreased rapidly when hydrogen peroxide was added to basic persulfate solutions (Figure 6), which confirms that hydroperoxide reacts rapidly with persulfate. Furthermore, rates of hydroperoxide decomposition increased with increasing NaOH concentrations. The stoichiometry of the reaction of hydroperoxide with persulfate is shown in Figures 7 and 8. The equivalent amounts of persulfate and hydrogen peroxide were added to the strongly alkaline solution, and both persulfate and hydroperoxide were decomposed at the same rate resulting in stoichiometry 1:1 (Figure 7). When 0.5 M hydroperoxide was added to 0.5 M persulfate, nearly all of the hydroperoxide was consumed over 150 min (Figure 8). However, when 1 M hydroperoxide was added to 0.5 M persulfate, the reaction stalled with ~0.5 M hydroperoxide remaining. These results confirm a molar ratio of approximately 1:1 for the reaction of hydroperoxide with persulfate.

Degradation of the reductant/superoxide probe hexachloroethane in NaOH:persulfate systems (2:1 molar ratio) with the addition of increasing hydroperoxide concentrations is shown in Figure 9. As the concentration of added hydroperoxide increased, hexachloroethane degradation increased proportionately. These results are consistent with the proposed mechanism

of the oxidation of hydroperoxide to superoxide as persulfate is reduced to sulfate and sulfate radical. Hexachloroethane degradation by superoxide proceeds in proportion to the mass of hydroperoxide added to the system.

Detection of Radicals. Previous studies have reported the generation of hydroxyl radical in alkaline persulfate systems *(28, 29)*. Hydroxyl and sulfate radicals were investigated in base activated persulfate reactions by using DMPO as a spin trap and DTPA to complex possible metal impurities in the system (Figure 10). Three DMPO radical adducts were observed in the ESR spectra (Figure 10): a hydroxyl radical adduct (DMPO–OH) with hyperfine splitting constants of A_N =14.57 and A_H = 14.57 and a sulfate radical adduct (DMPO–OH) with hyperfine splitting constants of A_N = 13.49, A_H = 9.77, $A^{\gamma_1}{}_H$ = 1.37, and $A^{\gamma_2}{}_H$ = 0.88–gauss. These results are consistent with ESR spectra and hyperfine splitting constants obtained for hydroxyl and sulfate radical in other studies (*28, 29*).In the proposed mechanism, hydroxyl radicals are formed as a result of reaction [6]. Superoxide was not detected during ESR analyses, likely because of its low reaction rate with DMPO-OH (k=10-18 $M^{-1}s^{-1}$) *(30, 31)*. Unlike hydroxyl radicals, for example, react with DMPO at significantly higher rate of k = 2.1-5.7×10^9 $M^{-1}s^{-1}$ in alkaline systems. Besides, superoxide radical is formed in low yield and scavenged by reactions [7] and [11] in the proposed mechanism. Therefore, the superoxide probe HCA was used to investigate the generation of superoxide in NaOH-persulfate reactions (Figure 11). Hexachloroethane degraded by 35% over 96 hours in systems containing a 3:1 molar ratio of NaOH:persulfate, and by 95% over 96 hours in systems containing a 6:1 molar ratio of NaOH:persulfate, demonstrating that superoxide is generated in persulfate systems under extremely alkaline conditions.

A mechanism for the base activation of persulfate was proposed in which 1) persulfate decomposes to hydroperoxide through alkaline hydrolysis, and 2) hydroperoxide reduces another persulfate molecule resulting in the formation of sulfate radical and sulfate; the hydroperoxide is then oxidized to superoxide.

Kinetic analysis of persulfate decomposition is consistent with its alkaline hydrolysis. Persulfate decomposition rates increased as a function of increased doses of sodium hydroxide. The reaction rate as a function of ionic strength provided further evidence of a nucleophilic attack in basic persulfate systems.

Hydroperoxide decomposition dynamics are also consistent with the proposed mechanism. One half mole of O_2 was produced per mole of persulfate decomposed, which agrees with stoichiometry of the proposed mechanism. Hydroperoxide reacts rapidly in basic persulfate systems, and cannot be detected because it is formed in low yields; furthermore, it reduces persulfate as soon as it is generated.

In summary all of the data collected to date are consistent with the proposed mechanism of alkaline hydrolysis of persulfate to hydroperoxide with subsequent reduction of another persulfate molecule by hydroperoxide. The mechanism explains the wide ranging reactivity of base-activated persulfate as the result of the generation of hydroperoxide, sulfate radical, hydroxyl radical and superoxide.

Literature Cited

(1) Watts, R. J.; Teel, A. L. Treatment of contaminated soils and groundwater using ISCO. *Pract. Period. Haz. Waste Manag.* **2006**, 2-9.

(2) Anipsitakis, G. P.; Dionysiou, D. D., Radical generation by the interaction of transition metals with common oxidants. *Environ. Sci. Technol.* **2004,** *38*, 3705-3712.

(3) Huang, K.; Zhao, Z.; Hoag, G.; Dahmani, A.; Block, P., Degradation of volatile organic compounds with thermally activated persulfate oxidation. *Chemosphere* **2005,** *61*, 551-560.

(4) Liang, C. J.; Bruell, C. J.; Marley, M. C.; Sperry, K. L., Persulfate Oxidation for in situ remediation of TCE. I. Activated by ferrous ion with and without a persulfate-thiosulfate redox couple. *Chemosphere* **2004,** *55*, 1213-1223.

(5) Liang, C. J.; Bruell, C. J.; Marley, M. C.; Sperry, K. L., Thermally Activated Persulfate Oxidation of Trichloroethylene (TCE) and 1,1,1-Trichloroethane (TCA) in Aqueous Systems and Soil Slurries. *Soil Sed. Contam.* **2003,** *12*, 207-228.

(6) Nadim, F.; Huang, K.; Dahmani, A., Remediation of soil and ground water contaminated with PAH using heat and Fe(II)-EDTA catalyzed persulfate oxidation. *Water Air Soil Pollut. Focus* **2006,** *6*, 227-232.

(7) Liang, C.; Bruell, C. J., Thermally activated persulfate oxidation of trichloroethylene: experimental investigation of reaction orders. *Ind. Eng. Chem. Res.,* **2008,** *47*, 2912-2918.

(8) Liang, C.; Wang, Z.-S.; Bruell, C. J., Influence of pH on persulfate oxidation of TCE at ambient temperatures. *Chemosphere* **2007,** *66*, 106-113.

(9) House, D. A., Kinetics and mechanism of oxidations by peroxydisulfate. *Chem. Rev.* **1962,** *62*, 185-203.

(10) Brown, R. A., Director of Technology, Development, Environmental Research Management. *Personal Communication* **2009**.

(11) Root, D. K.; Lay, E. M.; Block, P. A.; Cutler, W. G. *Investigation of chlorinated methanes treatability using activated sodium persulfate*, the First International Conference on Environmental Science and Technology, New Orleans, Louisiana, USA, 2005.

(12) Block, P. A.; Brown, R. A.; Robinson, D. *Novel activation technologies for sodium persulfate in situ chemical oxidation*, the Fourth International Conference on the Remediation of Chlorinated and Recalcitrant Compounds, Monterey, CA, USA, 2004.

(13) Singh, U. C.; Venkatarao, K., Decomposition of peroxodisulphate in aqueous alkaline solution. *J. Inorg. Nucl. Chem.* **1976,** *38*, 541-543.

(14) Kolthoff, I. M.; Miller, I. K., The chemistry of persulfate. I. The kinetics and mechanism of the decomposition of the persulfate ion in aqueous medium. *J. Am. Chem. Soc.* **1951,** *73,* 3055-3059.

(15) Martire, D. O.; Gonzalez, M. C., Kinetic evidence for the reaction of $O^{-\cdot}$ radical ions and peroxodisulfate in alkaline aqueous solutions. *Int. J. Chem. Kinet.* **1998,** *30*, 491-496.

(16) Das, K. C.; Misra, H. P., Hydroxyl radical scavenging and singlet oxygen quenching properties of polyamines. *Mol. Cell. Biochem.* **2004,** *262*, 127-133.

(17) Monig, J.; Bahnemann, D.; Asmus, K.-D., One electron reduction of CCl_4 in oxygenated aqueous solutions: a CCl_3O_2-free radical mediated formation of Cl^- and CO_2. *Chem. Biol. Interact.* **1983,** *47,* 15-27.

(18) Smith, B. A.; Teel, A. L.; Watts, R. J., Identification of the reactive oxygen species responsible for carbon tetrachloride degradation in modified Fenton's systems. *Environ. Sci. Technol.* **2004,** *38*, 5465-5469.

(19) Wahba, N.; El Asmar, M. F.; El Sadr, M. M., Iodometric method for determination of persulfates. *Anal. Chem.* **1959,** *31*, 1870-1871.

(20) Ossadnik, S.; Schwedt, G., Comparative study of the determination of peroxomonosulfate, in the presence of other oxidants, by capillary zone electrophoresis, ion chromatography, and photometry. *Fresenius J. Anal. Chem.* **2001,** *371*, 420-424.

(21) Eisenberg, G. M., Colorimetric determination of hydrogen peroxide. *Ind. Eng. Chem. Anal. Ed.* **1943,** *15*, 327-328.

(22) Cohen, I. R.; Purcell, T. C., Spectrophotometric determination of hydrogen peroxide with 8-Quinolinol. *Anal. Chem.* **1967,** *39*, 131-132.

(23) Furman, O.; Laine, D. F.; Blumenfeld, A.; Teel, A. L.; Shimizu, K.; Cheng, I. F.; Watts, R. J., Enhanced reactivity of superoxide in water-solid matrices. *Environ. Sci. Technol.* **2009,** *43*, 1528-1533.

(24) *The SAS system for Windows*, Release 9.1.; SAS Institute: Cary, NC, 2003.

(25) Ball, D. L.; Edwards, J. O., The kinetics and mechanism of the decomposition of Caro's acid.I. *J. Am. Chem. Soc.* **1956,** *78*, 1125-1129.

(26) Koubek, E.; Levey, G.; Edwards, J. O., An isotope study of the decomposition of Caro's acid. *Inorg. Chem.* **1964,** *3*, 1331-1332.

(27) Lunenok-Burmakina, V. A.; Aleeva, G. P., Mechanism of the decomposition of peroxomonosulphates and peroxomonophosphastes in alkaline aqueous solution. *Russ. J. Phys. Chem.* **1972,** *46*, 1591-1592.

(28) Davies, M. J.; Gilbert, B. C.; Stell, J. K.; Whitwood, A. C., Nucleophilic substitution reactions of spin adducts. Implications for the correct identification of reaction intermediates by EPR/spin trapping. *J. Chem. Soc., Perkin Trans. 2* **1992**, 333-335.

(29) Kirino, Y.; Ohkuma, T.; Kwan, T., Spin trapping with 5,5-Dimethylpyrroline-N-oxide in aqueous solution. *Chem. Pharm. Bull.* **1981,** *29*, 29-34.

(30) Finkelstein, E.; Rosen, G. M.; Rauckman, E. J., Spin trapping. Kinetics of the reaction of the superoxide and hydroxyl radicals with nitrones. *J. Am. Chem. Soc.* **1980,** *102*, 4994-4999.

(31) Keszler, A.; Kalyanaraman, B.; Hogg, N., Comparative investigation of superoxide trapping by cyclic nitrone spin traps: the use of singular value decomposition and multiple linear regression analysis. *Free Radical Biol. Med.* **2003,** *35*, 1149-1157.

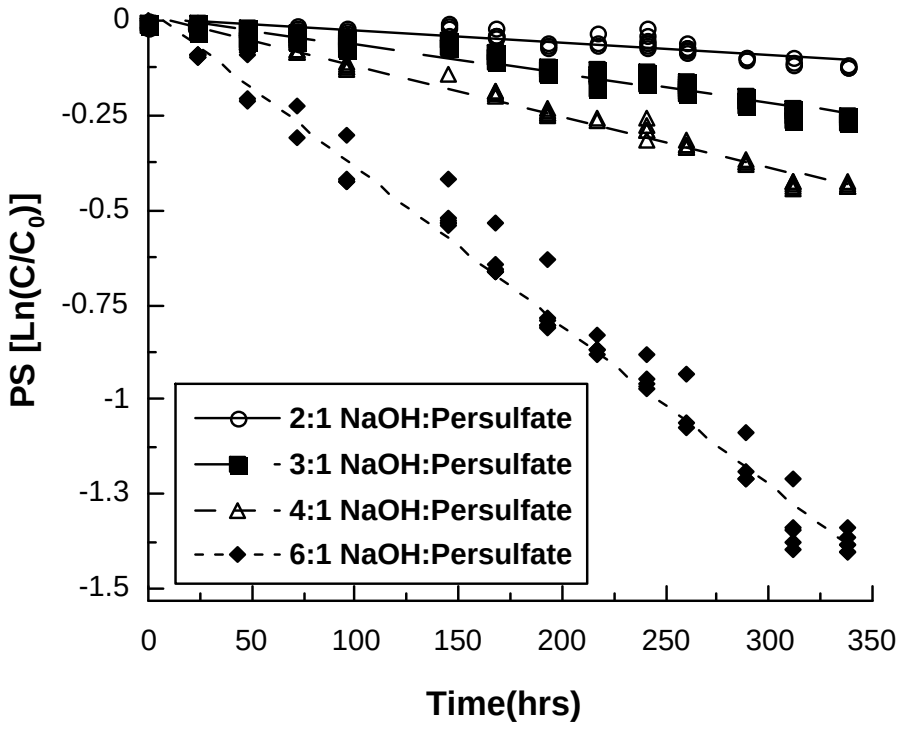

Figure 1. First order decomposition of base-activated persulfate with varying molar ratios of NaOH:persulfate (reactors: 0.5 M persulfate, 1 M, 1.5 M, 2 M, or 3 M NaOH; 20 mL total volume; T = 20 ± 2˚C).

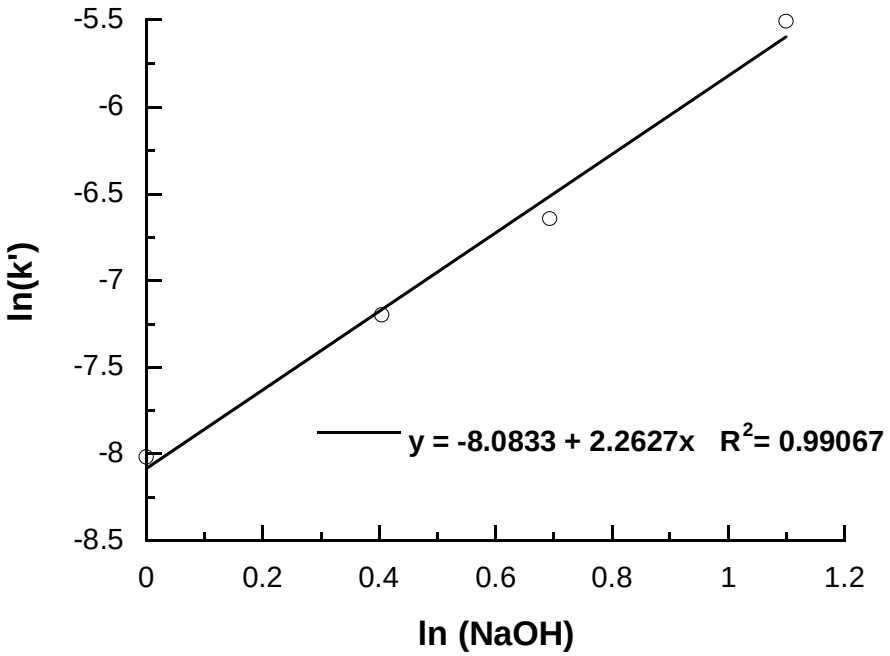

Figure 2. First order rate constants for persulfate decomposition in base-activated systems as a function of initial NaOH concentration.

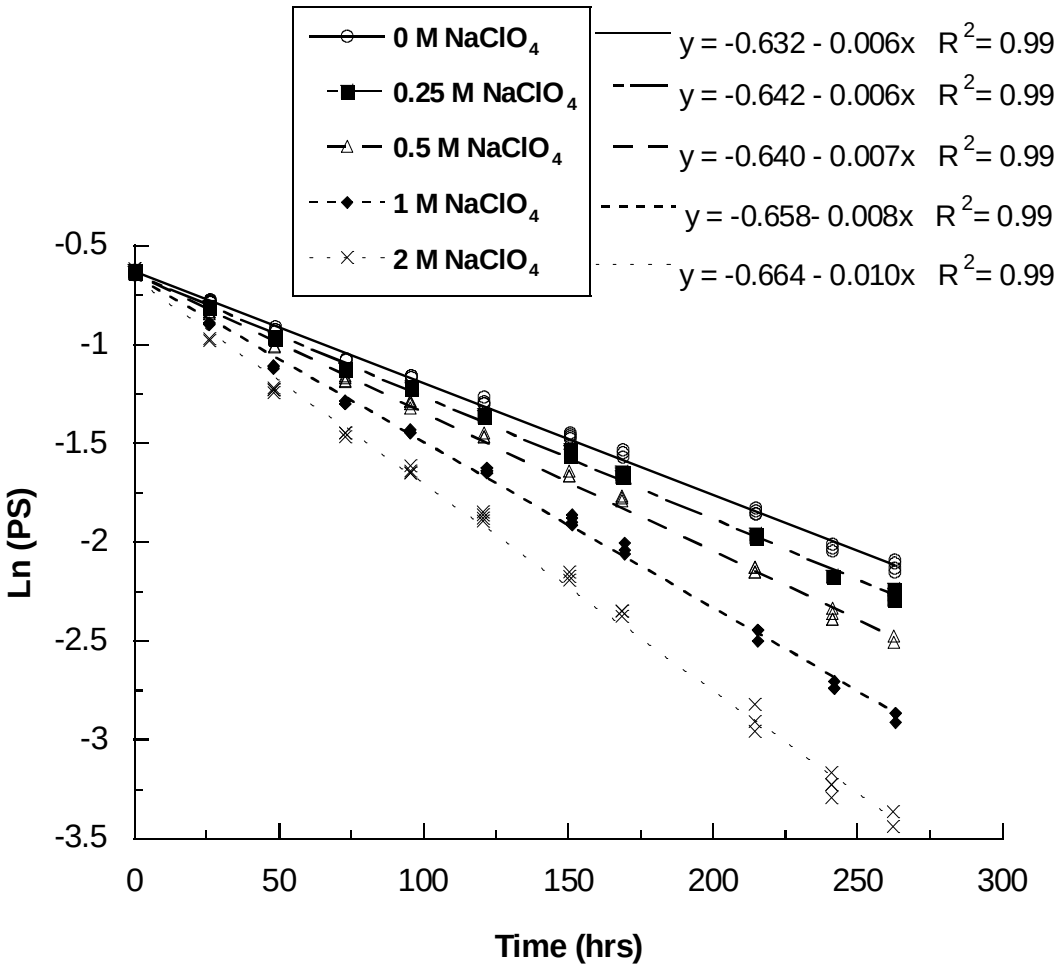

Figure 3. Effect of ionic strength on persulfate decomposition in base activated systems (reactors: 0.5 M persulfate, 3 M NaOH, 0–2 M $NaClO_4$; 20 mL total volume; T = 20 ± 2˚C).

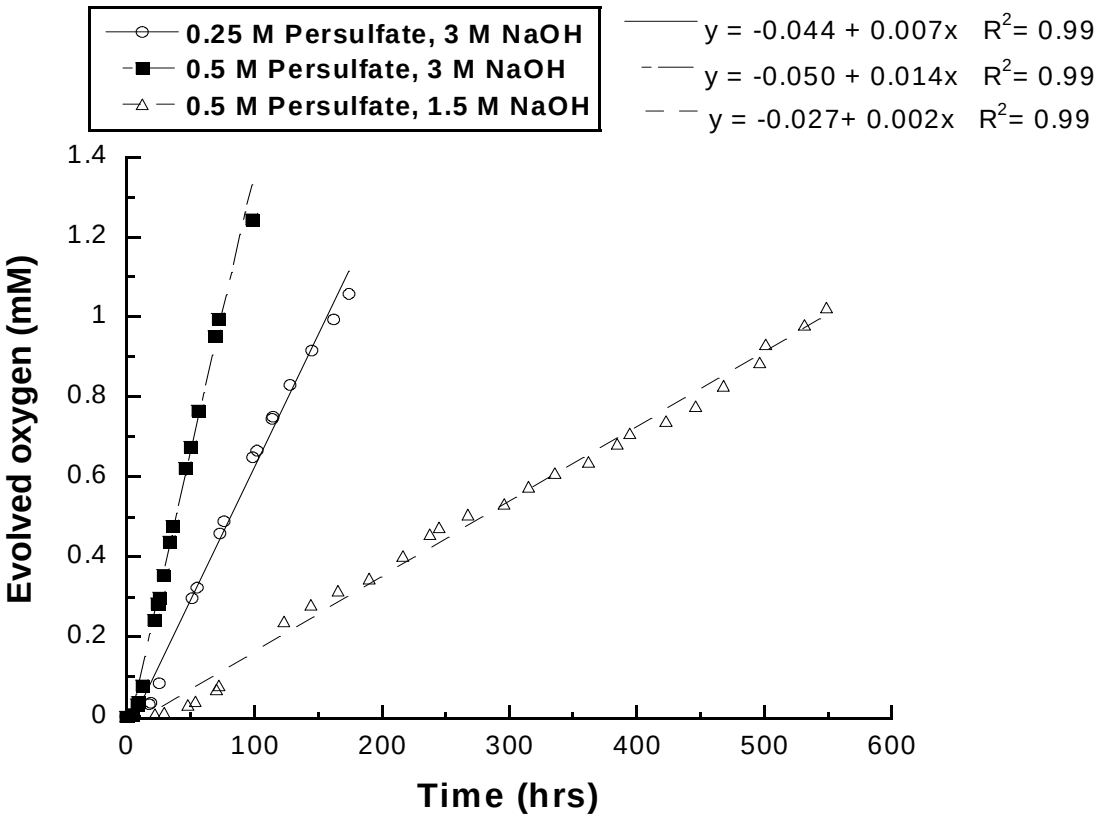

Figure 4. Evolution of oxygen over time in persulfate-NaOH reactions (reactors: 1) 0.25 M persulfate, 3M NaOH; 2) 0.5 M persulfate, 3 M NaOH; and 3) 0.5 M persulfate, 1.5 M NaOH; 12ml total volume; T = 20 ± 2˚C).

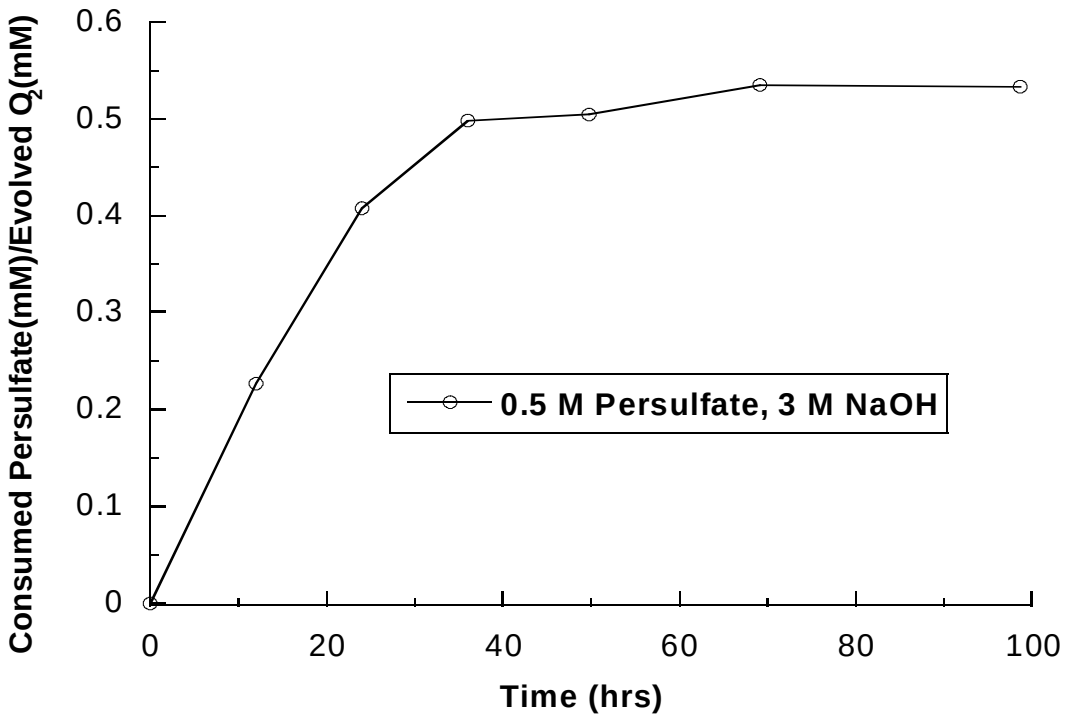

Figure 5. The ratio of consumed persulfate to generated oxygen over time in a base-activated persulfate system.

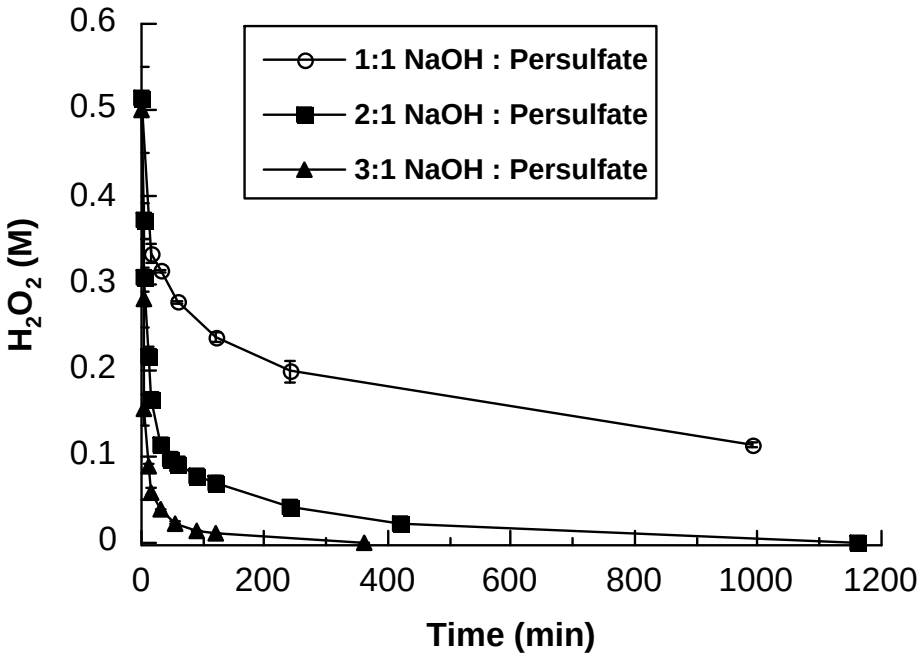

Figure 6. Decomposition of added hydroperoxide in base activated persulfate systems (reactors: 0.5 M H_2O_2, 0.5 M persulfate and 0.5 M, 1 M, or 1.5 M NaOH; 20 mL volume; T = 20 ± 2˚C).

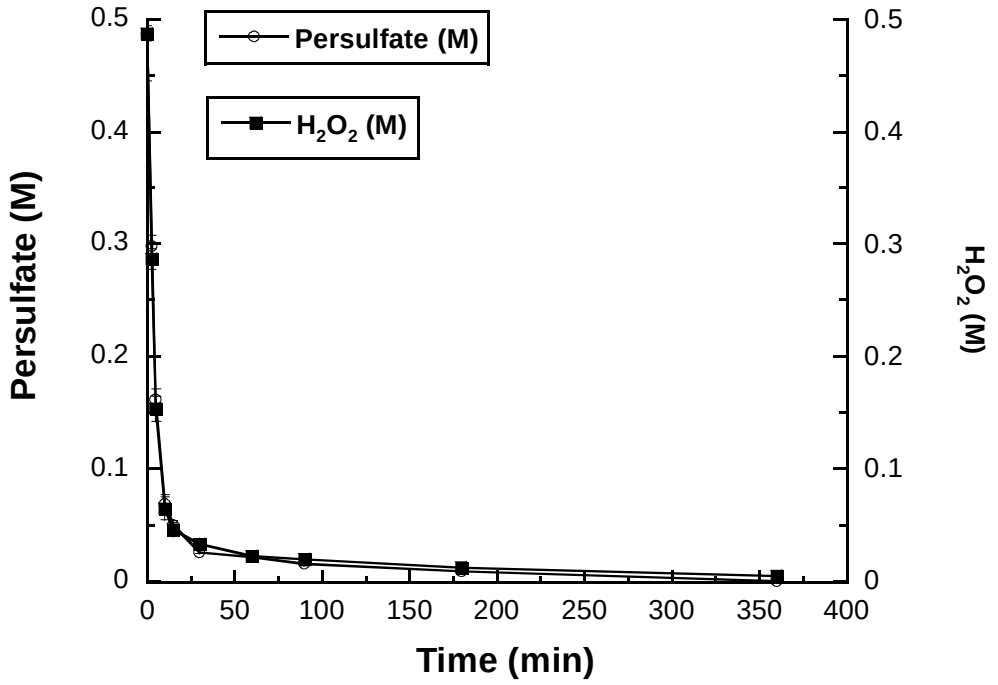

Figure 7. Decomposition of persulfate and hydrogen peroxide in 1:1 persulfate: H_2O_2 system (reactors: 0.5 M persulfate, 0.5 M H_2O_2, 1.5 M NaOH; 20 mL total volume; T = 20 ± 2˚C).

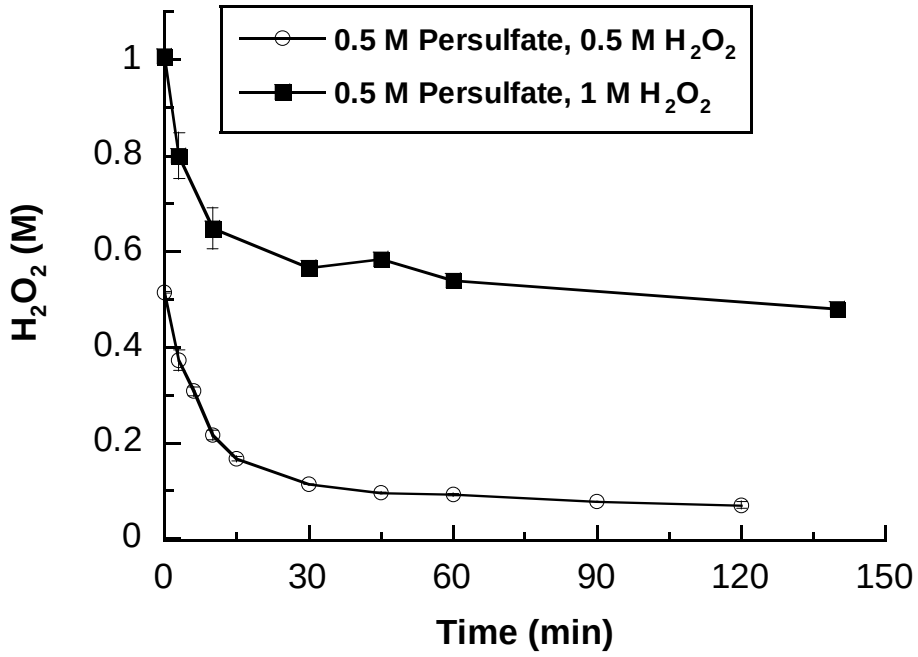

Figure 8. Stoichiometry for the degradation of added hydroperoxide in base activated persulfate systems (reactors: 0.5 M persulfate, 1 M NaOH, 0.5 M or 1 M H_2O_2; 20 mL total volume; T = 20 ± 2˚C).

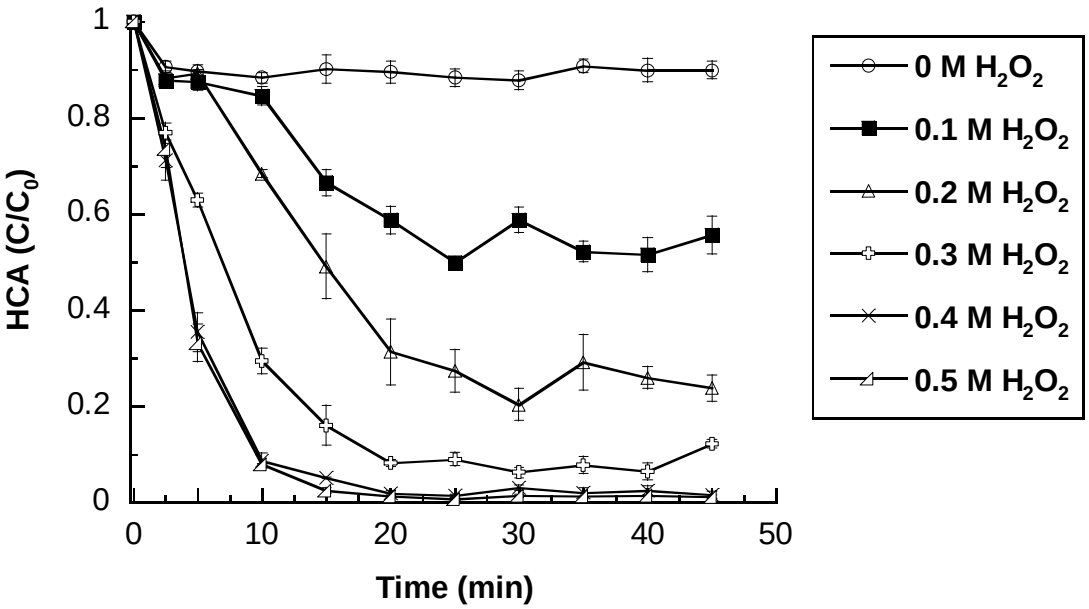

Figure 9. Relative rates of superoxide generation measured by the probe molecule hexachloroethane when hydroperoxide is added to base activated persulfate systems (reactors: 0.5 M persulfate, 1 M NaOH, 0–0.5 M H_2O_2, 2μM HCA; 20 mL total volume; T = 20 ± 2˚C).

(a) Control conditions: 0.1M NaOH, 0.005 M DTPA, 0.15M DMPO

(b) Reaction conditions: 0.05M $Na_2S_2O_8$, 0.1M NaOH, 0.005 M DTPA, 0.15M DMPO

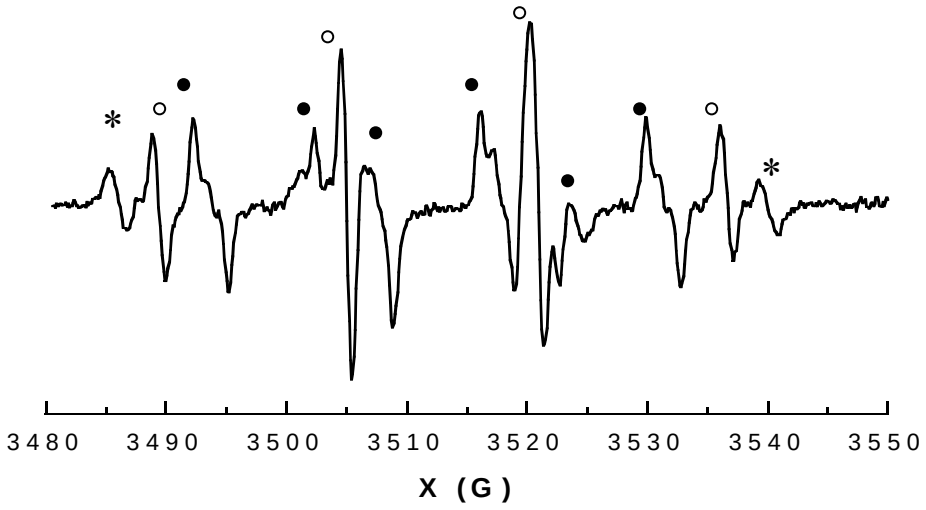

Figure 10. ESR spectra of DMPO•-OH (◦) and DMPO• -SO_4 (•) adducts and an unknown radical adduct (*) in a base-activated persulfate system (reactors: 0.05 M persulfate, 0.1 M NaOH, 5 mM DTPA, 0.15 M DMPO; 3 mL total volume; T = 20 ± 2˚C).

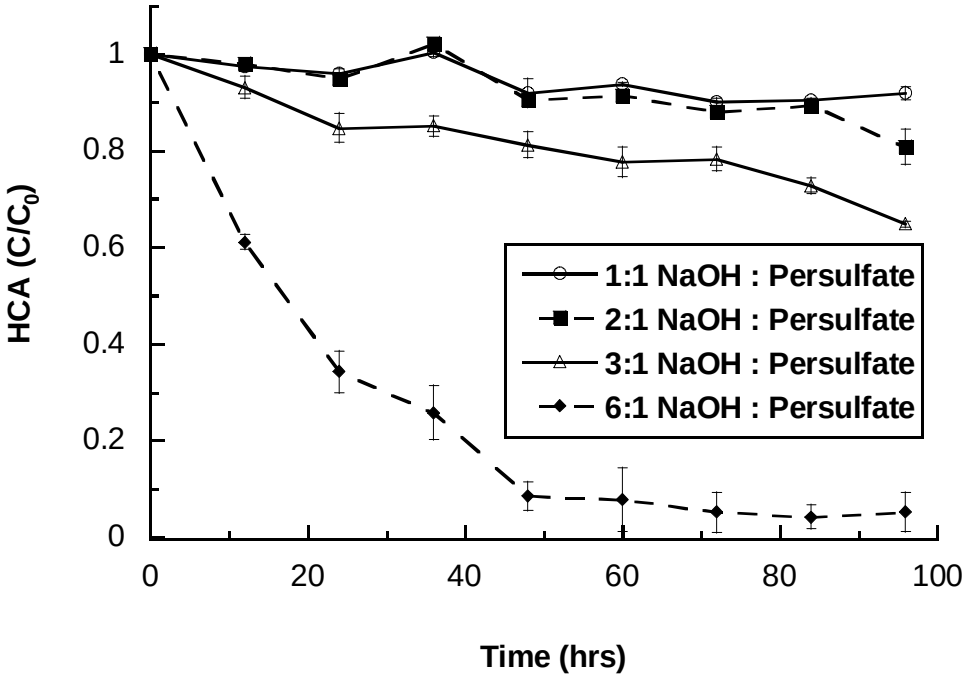

Figure 11. Degradation of the superoxide probe HCA in a base-activated persulfate system (reactors: 0.5 M persulfate, 0.5 M, 1 M, 1.5 M, or 3 M NaOH, 2 μM HCA; 20 mL total volume; T = 20 ± 2˚C).

APPENDIX 1

Supporting Information

Enhanced Reactivity of Superoxide in Water-Solid Matrices

The Eley-Rideal kinetic model was used to examine the reaction between superoxide and HCA in H_2O_2-birnessite system. Reactions 1-4 serve as the basis for the model.

$$H_2O_2 \underset{k_{-1}}{\overset{k_1}{\rightleftharpoons}} H_2O_{2sorbed} \qquad K_1 \qquad [1]$$

$$H_2O_{2sorbed} \underset{k_{-2}}{\overset{k_2}{\rightleftharpoons}} O_2^-{}_{sorbed} \qquad K_2 \qquad [2]$$

$$O_2^-{}_{sorbed} \xrightarrow{HCA} \text{Products} \qquad k_3 \qquad [3]$$

$$O_2^- \underset{k'_{-1}}{\overset{k'_1}{\underset{MnO_2}{\rightleftharpoons}}} O_2^-{}_{sorbed} \qquad K'_1 \qquad [4]$$

where K_1 = the adsorption coefficient for H_2O_2,
k_1 = sorption rate for H_2O_2,
k_{-1} = desorption rate for H_2O_2,
k_2 = decomposition of hydrogen peroxide with the formation of superoxide on the surface,
k_{-2} = dismutation rate for superoxide on the surface,
K_2 = equilibrium constant for the reaction [2],
k_3 = reaction rate for the reaction between superoxide and HCA,
K'_1 = the adsorption coefficient for superoxide,
k'_1 = sorption rate for O^-_2,
k'_{-1} = desorption rate for O^-_2,
The assumtions of the model are as follows: Reactions 1 through 4 take place at the catalyst surface, the initial rate of superoxide formation is proportional to the concentration of H_2O_2, and the concentration of superoxide is at steady-state.

Assuming steady-state conditions for superoxide:

$$k_2 \cdot [H_2O_2]_{sorbed} - k_{-2} \cdot [O_2^-]_{sorbed} - k_3 \cdot [O_2^-]_{sorbed} = 0 \qquad [5]$$

$$k_{-1}[H_2O_2]_{sorbed} = k_1[H_2O_2] \quad [6]$$

$$k'_{-1}[O_2^-]_{sorbed} = k'_1[O_2^-] \quad [7]$$

$$k_2 \cdot K_1 \cdot [H_2O_2] - k_{-2} \cdot K'_1 \cdot [O_2^-] - k_3 \cdot K'_1 \cdot [O_2^-] = 0 \quad [8]$$

$$[O_2^-] = \frac{k_2 \cdot K_1 \cdot [H_2O_2]}{K'_1 \cdot (k_{-2} + k_3)} \quad [9]$$

The Eley-Rideal mechanism for the reaction between sorbed superoxide and aqueous HCA may be expressed as:

$$rate = \frac{k_3 K'_1 [HCA] \cdot [O_2^-]}{1 + K'_1 [O_2^-]} \quad [10]$$

$$rate = k_3 \cdot [HCA] \cdot \theta_{O_2^-} \quad [11]$$

where $\theta_{o_2^-}$ is the surface coverage by superoxide,

$$k_{obs} = \frac{rate}{[HCA]} \quad [12]$$

$$k_{obs} = \frac{k_3 K'_1 \cdot [O_2^-]}{1 + K'_1 [O_2^-]} \quad [13]$$

Substituting equation [9] into equation [13]:

$$k_{obs} = \frac{k_3 K'_1 \cdot \frac{k_2 \cdot K_1 \cdot [H_2O_2]}{K'_1 \cdot (k_{-2} + k_3)}}{1 + K'_1 \cdot \frac{k_2 \cdot K_1 \cdot [H_2O_2]}{K'_1 \cdot (k_{-2} + k_3)}} \quad [14]$$

or

$$\frac{1}{k_{obs}} = \frac{1}{k_3 \cdot \frac{k_2 \cdot K_1}{(k_{-2} + k_3)} \cdot [\mathrm{H_2O_2}]} + \frac{1}{k_3} \quad [15]$$

APPENDIX 2

Persulfate Decomposition Kinetics

$^{-}{}_{3}OS\text{-}O\text{-}O\cdots SO_3^{-} + OH^- \xrightarrow{k_1} {}^{-}{}_{3}OS\text{-}O\text{-}O^- + HSO_4^-$ [1]

$^{-}{}_{3}OS\text{-}O\text{-}O^- + OH^- \longrightarrow H\text{-}O\text{-}O^- + SO_4^{2-}$ [2]

$H\text{-}O\text{-}O^- + {}^{-}{}_{3}OS\text{-}O\text{-}O\text{-}SO_3^- \xrightarrow{k_2} SO_4^{\bullet-} + HSO_4^- + O_2^{\bullet-}$ [3]

Persulfate decomposition follows two pathways through equations [1] and [3]:

$$\frac{-d[Na_2S_2O_8]}{dt} = k_1[Na_2S_2O_8][OH^-]^2 + k_2[Na_2S_2O_8][HO_2^-] = [Na_2S_2O_8]\left(k_1[OH^-]^2 + k_2[HO_2^-]\right)$$

$k_1 << k_2$, steady-state approximation for HO_2^-:

$$\frac{d[HO_2^-]}{dt} = k_1[Na_2S_2O_8][OH^-]^2 - k_2[Na_2S_2O_8][HO_2^-] = 0$$

$$[HO_2^-] = \frac{k_1[Na_2S_2O_8][OH^-]^2}{k_2[Na_2S_2O_8]} = \frac{k_1[OH^-]^2}{k_2}$$

Hence,

$$\frac{-d[Na_2S_2O_8]}{dt} = [Na_2S_2O_8]\left(k_1[OH^-]^2 + k_2\frac{k_1[OH^-]^2}{k_2}\right) = 2k_1[OH^-]^2[Na_2S_2O_8]$$